Review

Conservation of Architectural Heritage Structure Built with Tuff and Coral Rock: A Systematic Review of Geopolymer Formulation, Application, and Compatibility

Kent Benedict A. Salisid *, Raul Lucero Jr., Reymarvelos Oros, Mylah Villacorte-Tabelin, Theerayut Phengsaart, Shengguo Xue, Jiaqing Zeng, Ivy Corazon A. Mangaya-ay, Takahiko Arima, Ilhwan Park, Mayumi Ito, Sanghee Jeon, Carlito Baltazar Tabelin *

Posted Date: 2 March 2026

doi: 10.20944/preprints202603.0062.v1

Keywords: systematic literature review; architectural heritage structures; geopolymer; tuff; coral rock; architecture; heritage

 doi:10.20944/preprints202603.0062.v1

Review

Conservation of Architectural Heritage Structure Built with Tuff and Coral Rock: A Systematic Review of Geopolymer Formulation, Application, and Compatibility

Kent Benedict A. Salisid [1,2,*], Raul Lucero Jr. [1,2], Reymarvelos Oros [2], Mylah Villacorte-Tabelin [3,4], Theerayut Phengsaart [5], Shengguo Xue [6], Jiaqing Zeng [7], Ivy Corazon A. Mangaya-ay [8], Takahiko Arima [9], Ilhwan Park [9], Mayumi Ito [9], Sanghee Jeon [10] and Carlito Baltazar Tabelin [1,2,*]

[1] Department of Materials and Resources Engineering Technology, College of Engineering, Mindanao State University – Iligan Institute of Technology, Iligan City 9200, Philippines
[2] Resource Processing and Technology Center, RIEIT, Mindanao State University – Iligan Institute of Technology, Iligan City 9200, Philippines
[3] Center for Natural Products and Drug Discovery, PRISM, Mindanao State University-Iligan Institute of Technology, Iligan City 9200, Philippines
[4] Center for Microbial Genomics and Proteomics Innovation, PRISM, Mindanao State University-Iligan Institute of Technology, Iligan City 9200, Philippines
[5] Department of Mining and Petroleum Engineering, Faculty of Engineering, Chulalongkorn University, Bangkok 10330, Thailand
[6] School of Metallurgy and Environment, Central South University, Hunan 410083, China
[7] School of Metallurgy and Environment, Central South University, Changsha 410083, China
[8] College of Arts and Sciences, Bohol Island State University Main Campus, Tagbilaran, Bohol, Philippines
[9] Division of Sustainable Resources Engineering, Faculty of Engineering, Hokkaido University, Sapporo 060-8628, Japan
[10] Graduate School of International Resource Sciences, Akita University, Akita 010-0865, Japan
* Correspondence: kentbenedict.salisid@g.msuiit.edu.ph (K.B.A.S.); carlito.tabelin@g.msuiit.edu.ph (C.B.T.)

Abstract

Conservation of architectural heritage structures (AHS) requires compatible built heritage materials with aesthetic, physical, chemical, and mechanical properties similar to those of the original materials. In recent years, however, urbanization, land reclamation, depletion of stone quarries, anti-mining and anti-quarrying legislation have limited access to original heritage materials. In the absence of the original heritage materials, cement-based alternatives have been developed and widely applied for conservation. Major drawbacks of concrete- and cement-based materials include their large carbon footprint and long-term damage to the original rock or substrate, due to inadvertent promotion of salt efflorescence. This study systematically reviewed geopolymer-based materials as a sustainable, greener alternative to concrete- and cement-based materials for tuff- and coral rock-built heritage structures. The Preferred Reporting Items for Systematic Reviews and Meta-Analyses (PRISMA) guidelines were implemented for the literature review, using Scopus, Web of Science (WoS), and Google Scholar (supplementary) as databases, between 2013 and 2024. Inaccessible items, non-English, reviews, conference proceedings, book chapters, errata, and papers unrelated to geopolymers, tuff, and coral rock were excluded, resulting in a total of 103 articles. These works were classified into geopolymers (34 articles), tuff-built heritage structures (60 articles), and coral rock-built heritage structures (9 articles). This review included 103 items in the qualitative analysis; however, only 34 articles contained meaningful data for content analysis. These 34 articles were categorized in terms of the (i) main precursors; that is, metakaolin, fly ash, slag, and pyroclastic materials (i.e., pumice, volcanic ash, and volcanic soil), ceramic, others (i.e., tuff waste, silica fume, and mine wastes), (ii) formulations (i.e., precursors, activators, admixtures, and aggregates), and (iii)

 doi:10.20944/preprints202603.0062.v1

compressive strength. Furthermore, critical factors for compatibility were reviewed and classified into aesthetics (e.g., color, presence of efflorescence, and texture) and physical, chemical, and mechanical properties. This review also explored recent applications of geopolymers in heritage structures, indicating that geopolymers are typically used as repair mortar and consolidants. Finally, a bibliometric analysis was conducted to evaluate research trends on geopolymers, including a critical assessment of their aesthetic compatibility with heritage structures in the Philippines built with volcanic tuff and coral rock.

Keywords: systematic literature review; architectural heritage structures; geopolymer; tuff; coral rock; architecture; heritage

1. Introduction

Architectural heritage structures (AHS) are historical buildings, monuments, and sites constructed with natural stones or rocks as building materials, which are now being preserved for their cultural importance to future generations [1]. Many of these AHS were built using relatively soft rocks, with effective porosities of 20–60%, bulk densities of 1.0–2.5 g/m^3, and compressive strengths of 3–30 MPa. Two natural rocks commonly used in AHS are tuffs—a type of volcanic rock—and coral rock—a type of sedimentary rock—because they are locally available, soft enough to be worked with ancient tools, more durable than wood, and aesthetically beautiful.

Tuffs are rocks composed of pyroclastic materials (i.e., ash, rocks, and crystals) consolidated and naturally cemented with time due to extreme temperature and pressure generated during a volcanic eruption. They exhibit a variety of colors, textures, and physico-mechanical properties depending on their location [2]. Coral rocks are the exoskeletons of ancient corals, formed by the precipitation of aragonite (CaCO3) from dissolved calcium (Ca2+) and carbonate (CO32−) in shallow, tropical ancient marine ecosystems.

Table S1 lists some tuff-built AHS from different countries, along with their corresponding colors and physico-mechanical properties. In Europe, tuff-built AHSs are found in Italy, Hungary, Spain, the Netherlands, Slovakia, and Germany (Figure 1). In Italy, Naples had prominent AHS, such as the Ovo Castle, St. Elmo Castle, St. Domenico Maggiore Cathedral and St. Chiara constructed during the 13th–16th century using Neopolitan Yellow tuff, a yellowish-brown, lightweight, and low strength rock with a bulk density and compressive strength in the range of 1.0–1.3 g/m^3 and 3–6 MPa, respectively [4]. Meanwhile, a greyish-creamy to reddish-brown tuff with higher bulk density (1.6–1.8 g/cm^3) and compressive strength (7–26 MPa) than Neopolitan Yellow tuff was used to construct the Sirok Castle, Eger Cathedral, and Ottoman Minaret during the 13th–19th century in Hungary [5]. This tuff has a strength comparable to the greyish-beige tuff used in cathedrals, churches, and historical buildings in the Netherlands, with compressive strengths ranging from 13–29 MPa [6,7]. In Rochlitz, Germany, a slightly higher strength rock with a distinct deep reddish-brown color, having a similar appearance to a fired clay brick used to construct the Church of St. Maria in Mittweida, the Collegiate church in Wechselburg (Zchillen), and Portal of the church St. Kilian in Van Lausick, all of which were built around the 12th–15th centuries [8]. Similarly, a relatively high strength, pale green-grayish rock was utilized in Slovakia, in the Archaeological site of Mŏsnje during the 16th–19th century, [9] and the Arucas stones from Canary Island, Spain with a dominant grey and a hint of yellow, blue, and red was used in constructing the Church of San Juan Bautista has highest strength rock ranging from 50 to 100 MPa [10,11].

 doi:10.20944/preprints202603.0062.v1

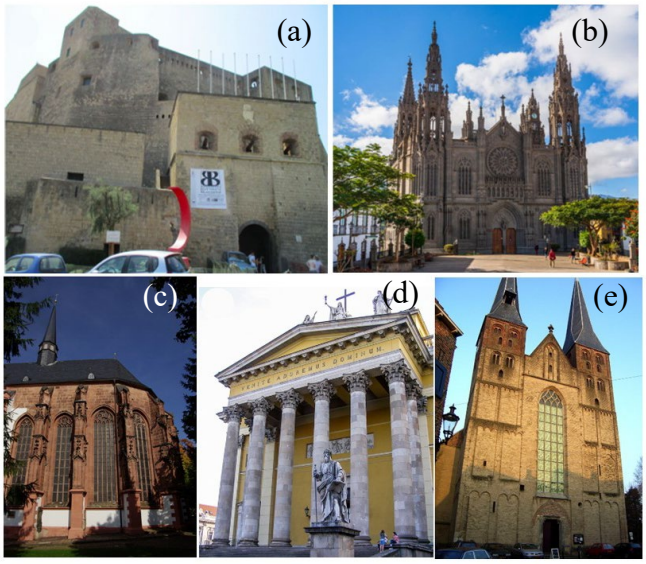

Figure 1. Examples of European tuff-built AHB: a) Ovo Castle, Naples, Italy (13th-16th century) [110], b) Church of San Juan Bautista, Canary Islands, Spain (20th century) [10], c) Church of St. Maria, Mittweida, Germany (15th century) [8], d) Eger Cathedral, Eger, Hungary, (19th century) [5], and e) Bergkerk, Deventer, Netherlands, (13th century) [7].

In North America, several AHS were constructed in Mexico in the 16th century during the Spanish occupation, and in Honduras during the Mayan civilization, dated 250–900 CE (Figure 2). In Mexico, there are a large variety of tuffs used in Spanish influenced AHS [12,13], two of the most popular are the "Piera Vieja", a pink-colored tuff with an effective porosity of 26.5%, bulk density of 1.8 g/cm^3 and compressive strength of 30.8 MPa, and "Barranca Tuff", with an effective porosity of 37.5%, and bulk density of 1.5 g/cm^3, which were used as building stones for Cathedrals in Morelia, and Aguascalinetes, respectively. Similarly, other colored tuffs were used, including the green-reddish colored "Loseros tuff", with an effective porosity of 6–17%, bulk density of 2.1–2.3 g/cm^3, and compressive strength of 21–74 MPa and the white-colored "Tezoantla tuff", with an effective porosity of 14.9%, bulk density of 1.9 g/cm^3, and compressive strength of 50–67 MPa used in the several historical site of Guanajuanto, and Hidalgo, respectively, to construct historical churches, cathedrals, and government buildings in Mexico [3,14–17]. In Honduras, the famous Heritage Site, the Archeological Site of Copan, with a classic Mayan architecture, such as the Hieroglyphic Stairway, was built using Maya Tuff during 756 CE, a buff-greenish-colored stone with an effective porosity of 27–28% [18,19].

 doi:10.20944/preprints202603.0062.v1

Figure 2. Examples of representative tuff-built AHS in North Americas: (a) Cathedral of Morelia, Mexico, (17th century) [14]; (b) Cathedral of Aguascalinetes, Mexico (16–20th century) [3]; (c) Façade of Santa Veracruz Chapel of Mineral del Monte, Mexico (16th century); (d) Façade of Legislative office, Loseros, Mexico, 19th century; and (e) Maya tuff stones, in Archeological Site in Copan, Honduras, (763 CE) [18,19].

In West Asia, several AHS were built in Turkey and Armenia using tuff (Figure 3). In Turkey, there are various types of tuffs but those quarried in the Cappadocia region [20] like the cream-beige colored Döğer Tuffs in Afyonkarahisar (effective porosity of 42%, bulk density of 2.5 g/cm3, and compressive strength of 26.5 MPa) [21–25], and whitish-gray tuff in Malatya (effective porosity of 14.8%, bulk density of 1.8-1.9 g/cm3, and compressive strength of 12.9 MPa) [26] are the most notable. These tuffs were used to construct caravanserai—a roadside inn alongside the Silk Road with a central courtyard used by travelers for trade and commerce—mosques, and churches such as the Kayseri Castle (527-565 B.C.) in Kayseri, and Döğer Caravanserai (1434) in Afyonkarahisar, and the 12th-century Battalgazi Mosque in Malatya. In Armenia, the tuff had a variety of colors, including black, red, golden, grey brown, and was used in the construction of religious monuments and buildings like the Cathedral of Etchmiadzin (constructed around 301–303 A.D.) and the All Savior Church in Gyumri, which was rebuilt using black tuff [27].

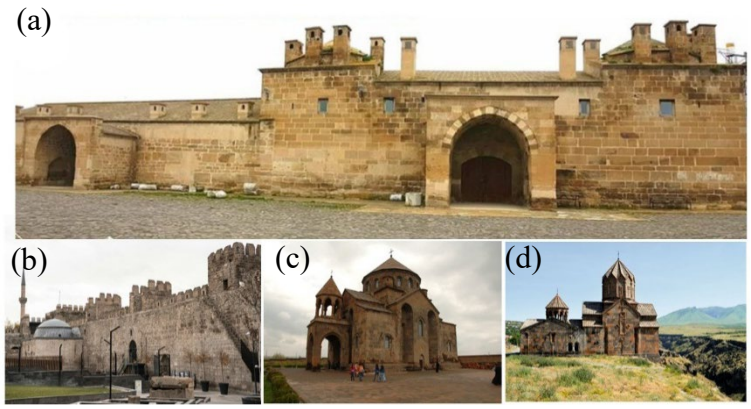

Figure 3. Examples of tuff-built AHS: (a) Döğer Caravanserai, Afyonkarahisar, Turkey (1434) [23], (b) Kayseri Castle, Kayseri, Turkey, (527-565 BC) [20], (c) Cathedral of Etchmiadzin (301-303 A.D), Armenia, and (d) All Savior Church, Gyumri, Armenia (1858-1872) [27].

In East Asian countries such as China, Japan, and South Korea, tuff was used to construct platforms for temples, pagodas, shrines, and sculpted statues, which generally had a common grayish hue as a distinguishing characteristic (Figure 4). In China, for example, Guo et al. [29] characterized the stone platform used in Baoguosi Temple, located in Ningbo, dated from 880–1013 C.E., having a light purple to grey color, which was similar to the tuff used in the Sanlao Stone chamber in Hangzhou, Zhejiang Province, with a grey-green color built in 1921 [30]. Meanwhile, in South Korea, the stones used in the five-story pagoda at Geumgolsan Mountain (Korean Treasure No. 529), in Jingdo-gun, are estimated to have been constructed in 918-1392 CE and originally had a yellow to light gray color but now appear black and brown from weathering [31]. Meanwhile, the Oya Stone, a soft tuff in Japan, can appear grayish, brownish/creamy, or greenish, and was used to build the famous Oya-ji temple in 810 CE [32,33].

 doi:10.20944/preprints202603.0062.v1

Figure 4. Examples of tuff-built AHS in East Asia: (a) Baoguosi Temple, Ningbo, China, (880–1013) [28], (b) Sanlao Stone House, Zhejiang, China (1921) [30], (c) Korean Treasure 529, Jingdo, S.Korea (918–1392 CE) [31], and (d) Oya-ji Temple, Kanto, Japan (810 CE) [32].

Another type of rock widely used for AHS is coral rock, also known as "coral stone" or "coral reef limestone". Coral rock is a type of limestone formed from coral reefs in ancient oceans, with an appearance similar to that of corals. They are formed when corals—produced by a multicellular organism called polyps—slowly develop a thick calcareous exoskeleton from sorbing abundant calcium (Ca^{2+}) and carbonate (CO_3^{2-}) ions in marine ecosystems. As these polyps die, their hard exoskeletons, consisting of calcium carbonate ($CaCO_3$), remain and, over millions of years, are buried, cemented, and compacted, transforming into coral rocks [34].

Table S2 summarizes some coral rock-built AHSs from the Maldives, Philippines, India, Mexico, Saudi Arabia, Iran, Kenya, and Tanzania. Like tuff, coral rocks come in several forms. For example, Meng et al. [35] reported four (4) categories of non-porous coral rocks—boulder, framework, gravel, and calcarenite—depending on the grain sizes (Figure 5). This variation in coral rock grain sizes could be attributed to the extent of dolomitization, cementation, erosion, and dissolution of coral skeletons over millions of years [35]. For example, the calcarenite coral rock used in constructing the Ramanathaswamy Temple (India) had a bulk density of 2.21 g/cm3 and a 50–60 MPa compressive strength [34].

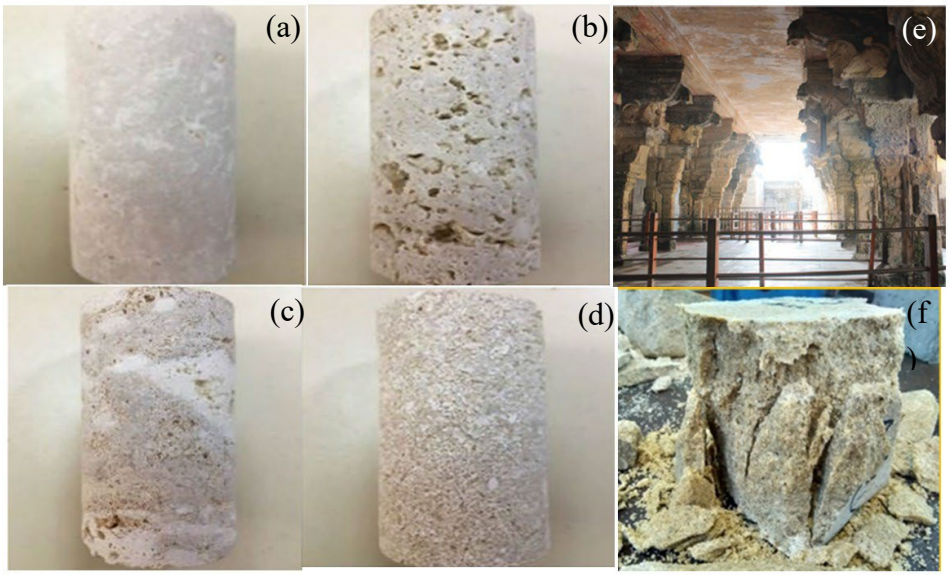

 doi:10.20944/preprints202603.0062.v1

Figure 5. Categories of non-porous, structured coral rocks: (a) boulder, (b) framework, (c) gravel, and (d) calcarenite [35]. Some examples of coral rocks in AHSs (e) Interior of Ramanthaswamy Temple, India, and (f) crushed coral rock, resembling calcarenite in Ramathaswamy Temple [34].

When the coral rocks have a reef-like appearance with visible pore structure, they can be classified into coarse-pore and fine-pore types, with annular and linear pore arrangements, respectively (Figure 6). Xu et al. [36], for example, employed a polarizing microscope and estimated pore sizes of 0.5–1 mm and 100–200 μm for coarse and fine coral rock, respectively. Wei et al. [37] also noted the lower compressive strengths (around 1.6–4.7 MPa) for coarse coral rock compared with fine coral rocks (around 7.6–15.1 MPa). Several examples of coarse coral rock are the Megalithic Temples of Malta, the Historical Houses of Jeddah in Saudi Arabia, the Historical Dome in Qeshm Island, Iran, and the Veracruz Port in Veracruz City, Mexico. In comparison, fine-pore coral rock was used in the Mosque in the Maldives, Historical Ruins in Kenya, Historical Houses in Tanzania, and Baroque Churches and Watchtowers in the Philippines.

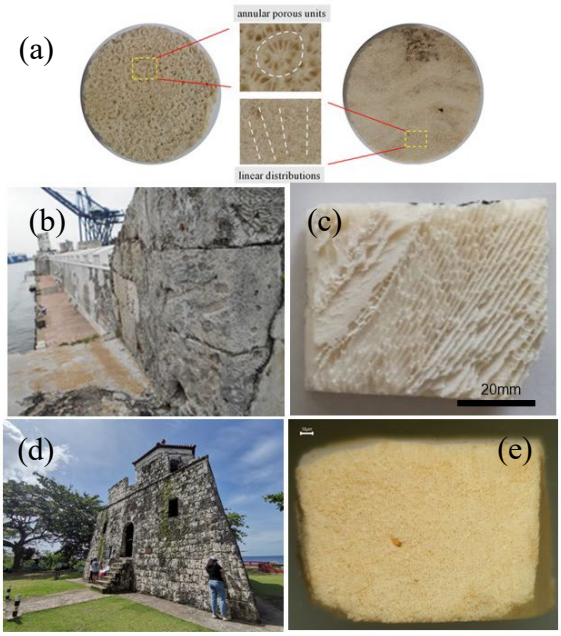

Figure 6. Different pore-structured coral rocks having a clear difference in pore structure: (a) coarse-pore coral rock and fine-pore coral rock [38], (b) coral rock used in the Port of Veracruz, Mexico [39], (c) 5-cm cubic specimen of coarse-pore coral rock in Port of Veracruz, Mexico, (d) Maribojoc Watchtower, Bohol, Philippines, and (e) 2-cm cubic specimen of fine-pore coral rock in Maribojoc Watchtower.

However, tuff and coral rocks are susceptible to weathering, resulting in visible material loss and degradation after prolonged exposure to the environment. For example, Seigesmund et al. [38] reported that scaling and flaking on the surface of tuffs used in Mexican and Armenian AHS were caused by swelling clay minerals that expand and contract during wet-dry cycles, inducing rock breakage and spalling due to internal tensile stresses. Similarly, Çelik and Sert [22] attributed the deterioration of tuff used in Turkish AHS to salt crystallization, which was promoted by the high volume of micropores (<0.1 μm in diameter) serving as nucleation sites for rapid salt crystal growth.

In comparison, coral rocks have higher resistance to salt weathering in comparison to Tuff due to their highly porous structure, but are susceptible to water erosion and acid-promoted dissolution attributed to dissolved CO_2 in the air that lowers the pH of rainwater to around 5.8 [117], which gradually dissolves $CaCO_3$ in limestones and coral rocks. Manohar et al. [34], for example, investigated the deterioration mechanism of coral rocks used in Ramanathaswamy Temple, Remeshwaram Island, India, and found insignificant mass loss even after 15 cycles of salt weathering tests, which was attributed to the large pore size of the rock (~70% are >0.5 μm). However, visible

 doi:10.20944/preprints202603.0062.v1

damage to coral rocks was observed due to erosion from rainwater seepage and wind. Similarly, Urbina Leonor et al. [39] assessed the deterioration pattern of coral rocks used in the Port City of Veracruz, Mexico using three (3) artificial rain solution, with pH of 5.0 (acid), 6.2 (non-acid), and 5.2 (global) consisting of [H^+], [Na^+], [NH_4^+], [K^+], [Mg^{2+}], [Ca^{2+}], [F^-], [Cl^-], [NO_3^-], [SO_4^{2-}], [HCO_3^-] or [CO_3^{2-}] and found that high precipitation volume promoted higher deterioration of the coral rock regardless of its acidity.

Figure 7 shows the locations of some AHBs constructed from tuff and coral rocks, indicating that most tuff-built AHBs are in areas with volcanoes, such as Japan, China, the Philippines, and Korea, all within the Pacific Ring of Fire. In addition, tuffs can be classified in terms of color depending on location, with tuffs found in South America (Mexico and Honduras) being light-colored, those found in Europe (e.g., Turkey) having grey to dark colorations, and those in Asian countries being characterized by intermediate (grey) to light colors. In comparison, AHS made of coral rocks are situated in coastal regions (i.e., ports or islands) in tropical countries and can be further classified based on their physical property; that is, fine-pore coral rocks in AHS are found in the Philippines, Kenya, Tanzania, and Maldives, coarse-pore coral rocks are common in AHS of Mexico (South America), Jeddah, Iran (Middle East) and Malta (Europe), and non-pored coral rocks such as the calcarenite coral rock in India.

Figure 7. World Map showing the location of some notable AHS built from tuff or coral rocks.

According to the International Council on Monuments and Sites (ICOMOS, 2003), the materials for AHS conservation must have visual and mechanical properties similar to those of the original materials to maintain historical authenticity and prevent damage. Traditional restoration materials for AHS use stones exploited from original historical quarries [8–10]. For example, Siedel et al. [8] reported that Rochlitz tuff, obtained from active quarries in the Rochlitz Mountain, was still used to restore historical structures in Germany. As reported by Cárdenes et al. [10], three (3) active quarry areas in Arcuas have been exploiting stones for the restoration of heritage structures in the Canary Islands and Spain. However, finding suitable materials for heritage conservation is becoming increasingly challenging due to rock depletion and the inaccessibility of historical quarries. One alternative approach is to find replacement or substitute stones that have similar properties to the rock substrate but are obtained from other quarry sites. For example, the Cathedral Basilica of Aguascalientes, Mexico [15] was built using a light pink tuff called Barranca tuff, but because of the depletion of historical quarries, several restoration efforts have used Valladolid tuff. More recently, commercially available dark, pink-colored tuffs have been used for the restoration of this cathedral.

 doi:10.20944/preprints202603.0062.v1

Although the original and replacement stones have a similar visual appearance, their formation times differ, resulting in differences in physico-mechanical properties and weathering behavior. For example, Blows et al. [40] reported that the currently unavailable Caen stone, a cream-colored, fine-grained French limestone formed during the Middle Jurassic period, used as a building material for heritage cathedrals in the United Kingdom, has often been replaced by Lepine stone, a whitish English limestone formed during the Upper Jurassic. Both stones were tested for salt weathering, and it was found that Lepine stone was less durable (14% mass loss) than the original Caen stone (4% mass loss) after 15 cycles of simulated salt weathering. These authors attributed the higher durability of Caen stone to its lower microcrystalline calcite content (50%) than that of Lepine stone (70%). Similarly, Přikryl and Török 2010 [41] assessed the impacts of a new stone introduced to the Charles Bridge in Prague, Czech Republic, which was built using local sandstone that is now unavailable due to the closure of all sandstone quarries in Prague. The color, physical, mechanical, and weathering behaviors of the new stone differed from those of the original substrate, which likely accelerated the deterioration of the Charles Bridge. As countermeasures, both the original and replacement stones were investigated based on their petrophysical and mechanical properties to determine their compatibility, rather than solely relying on visual characteristics such as color, texture, and grain size. Rozenbaum et al. [42] also emphasized selecting replacement stone based on its aesthetic, physical, and mechanical properties. These authors noted that Saint-Maximin stone, a French limestone used in Le Mans Cathedral (11th-15th century), was incompatible with Romanian Limestone in terms of composition (SiO2 of 12.5% and 0%; CaCO3 of 87.4% and 97.1%), total porosity (38.0 and 27.0), and pore volume sizes (18 μm and 8 μm). In comparison to Garchy Stone, a limestone originating from south Paris, used in the cathedrals in Orleans, Nevers and Bourges (13th century) and its compatible replacement limestone in central Romania having similar composition (SiO2 of 0 and 1.7%, $CaCO_3$ of 99.6% and 97.5%), total porosity (19.7%, and 18.2%), and pore volume sizes of (1.3 μm and 1 μm). Meanwhile, Martínez-Martínez et al. [3] followed the recommendation of Rozenbaum et al. [42] and investigated other replacement tuff stones of the original rocks used in AHS in Morelia from other quarries, which conducted compatibility tests based on petrophysical rather than solely aesthetic considerations.

Historically, conservation activities for AHS have relied on cementitious materials, such as cement- and concrete-based materials, due to their favorable mechanical properties and on-site applicability. In the 1950s, for example, concrete was used for the early restoration of Eger Castle in Hungary [43]. Concrete, however, promoted the formation of salt efflorescence, which led to severe deterioration of the original stone substrate. According to Török et al. [43], the lower permeability of the concrete sealing the tuff walls of the Eger Castle not only introduced more rainwater into the tuff substrate but also prevented pore-water evaporation, thereby enhancing salt efflorescence formation.

To improve compatibility, “artificial stones”, a type of concrete designed to mimic the natural physical and mechanical properties, including color and texture, of the natural stone by mixing local materials (e.g., natural pozzolana, crushed stones, local soils, sand) with white cement, superplasticizer, and inorganic-colored pigments, have recently been developed. For example, Stefanidou et al. [44], formulated an artificial stone to restore three (3) AHS in Greece, namely, Ancient Agora of Pella, (4th-5th BC), Ancient Theatre of Maronia (4th-3rd BC), and Fortress of Saint Nicolaos of the Medieval City of Rhodes (15th century) built from marl limestone, limestone/marble, and sandstone, respectively result showed compatibility to natural stones attributed to texture, color, pore size distribution and compressive strength. Similarly, Menningen et al. [28] developed an artificial stone to mimic the aesthetic appearance and petrophysical properties of the original Armenian Tuff for the restoration of cultural heritage, using cement, crushed original stones, and colored pigment. However, the drawbacks of artificial stone include the use of ordinary Portland cement (OPC), a major contributor to carbon dioxide (CO_2) emissions.

A more sustainable and eco-friendlier alternative for cement- and concrete-based materials is geopolymers, which are promising for the conservation of AHS [45,46]. Geopolymers have been widely used as a sustainable alternative to OPC for reducing carbon emissions, providing high

 doi:10.20944/preprints202603.0062.v1

chemical resistance and mechanical strength under optimal conditions [47–49], and repurposing waste streams [64–66]. For example, Amar et al. [50] obtained a higher 7-day unconfined compressive strength (UCS) of 44 MPa for geopolymer concrete in comparison to OPC concrete (36 MPa), while at later stages of hardening (28 days), both have comparable UCS of 51 MPa for geopolymer and 54 MPa for OPC.

Several review papers about heritage conservation have been published, but many did not focus on the application of geopolymers [116]. Among the few that included geopolymers in their reviews, the focus was limited to functionalizing geopolymers as coating mortars [45] and reinforcing historical structures [46]. These previous review papers also did not include compatibility criteria or issues between conservation materials, such as geopolymers, and the substrate or original materials of AHS in terms of aesthetics, chemical composition, physical attributes, and mechanical properties. This knowledge gap on heritage conservation is addressed in this work, which is guided by the following research questions:

i. What types of geopolymers have been applied for stone AHS conservation from 2013–2024?
ii. What are the compatibility criteria used in the application of geopolymers for cultural heritage conservation?
iii. What are the recent applications of geopolymers in stone AHS conservation?

2. Review Methodology

2.1. Search and Identification

This paper employed the Preferred Reporting Items for Systematic Reviews and Meta-Analyses (PRISMA) guidelines [52] and the protocols recommended by Andrews [53] to review the conservation of heritage structures built with tuff and coral rock using geopolymers. Prior to the search, the protocol was pre-registered in the Open Science Framework (OSF) with registration DOI: 10.17605/OSF.IO/RQMJU. The search criteria used the keywords “Geopolymer”,”coral rock”, “tuff” and “heritage,” with publication dates restricted to 2013-2024, across the Scopus and Web of Science (WoS) databases. A total of 487 items, 227 from Scopus and 260 from WoS, were retrieved, which were reduced to 368 after removing duplicates.

2.2. Screening and Inclusion Criteria

Figure 8 shows the screening process, which excluded articles that did not focus on tuff, coral rocks, or geopolymers based on titles, abstracts, highlights, and keywords. These criteria removed 249 articles, resulting in 119 items for eligibility assessment. Based on the eligibility criteria, conference proceedings (13), inaccessible articles (2), review papers (1) and non-English (1) were removed. Full-text articles were also evaluated [54], and those not focusing on geopolymers for AHS conservation (9) were excluded. The PRISMA Guidelines also allow the inclusion of articles using other methods; thus, 10 articles were added using Google Scholar following the same screening criteria, and a total of 107 articles were classified for content analysis (Figure 9). Because this review focuses on geopolymers for heritage conservation, quantitative analysis was done using 34 papers that contained suitable data sets, while the remaining 69 articles related to tuff and coral rock-architectural built heritage (69) were used for qualitative analysis. The 34 geopolymer papers were further subdivided into different precursor materials used: (i) metakaolin (12), fly ash (4), slag (4), volcanic ash (5), ceramic wastes (4), tuff waste (1), pumice (1), silica fume (1), local clay (1), and mine wastes (1).

 doi:10.20944/preprints202603.0062.v1

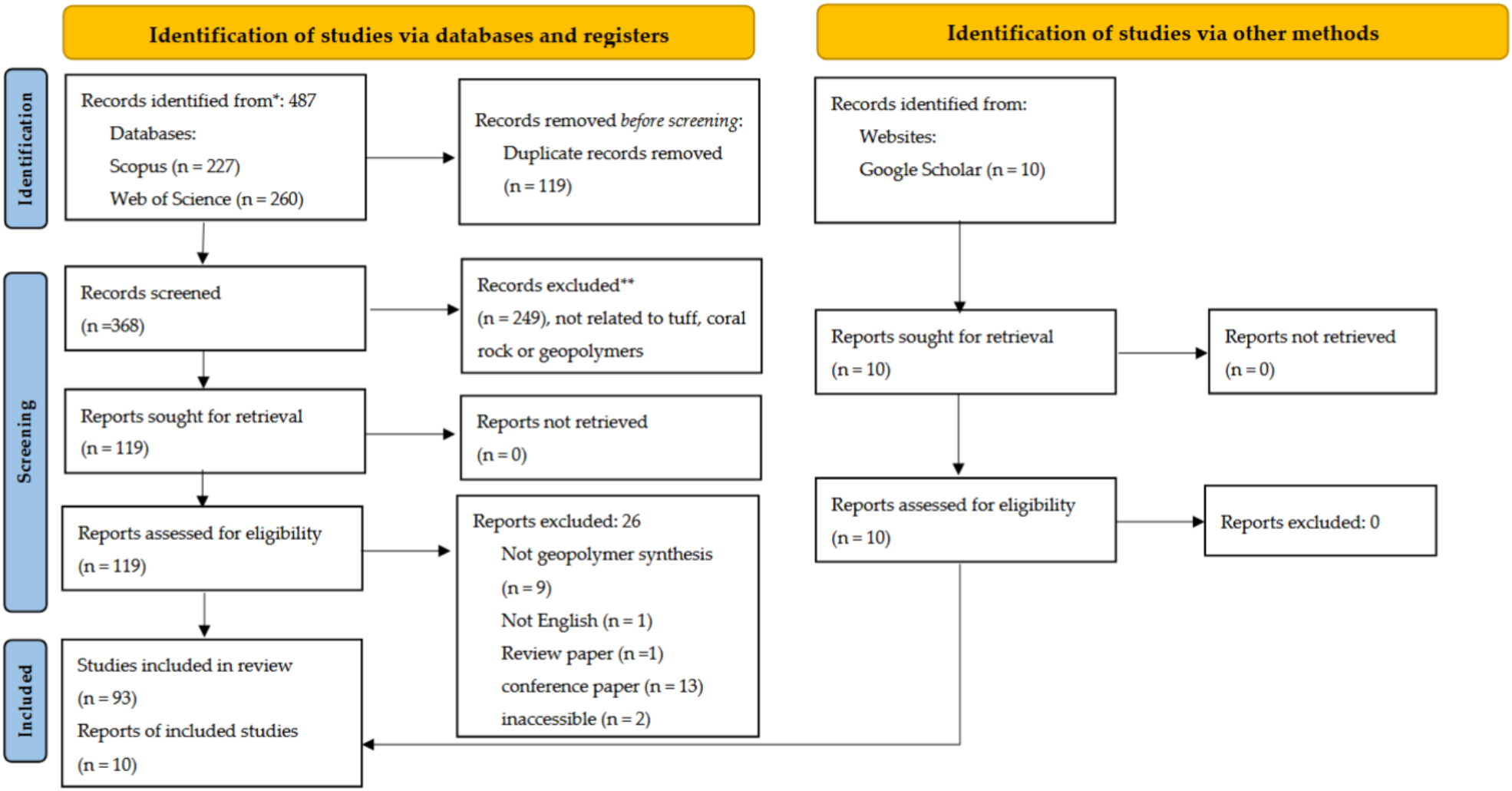

Figure 8. A schematic diagram of the article selection process following the PRISMA Guidelines.

 doi:10.20944/preprints202603.0062.v1

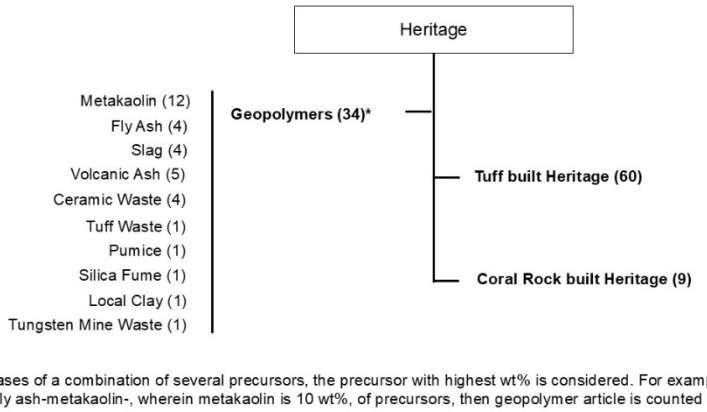

Figure 9. Classification of eligible items related to AHS conservation analyzed in this review.

2.3. Publication Trends

Figure S10 displays the trend of 34 articles on geopolymers for heritage conservation with more discussion can be found as supplementary information.

2.4. Active Countries, Journals, and Institutions

Table S3 lists the countries where research on geopolymers for heritage conservation is active. Italy has the highest frequency on the list at 50%,

Figure S11a shows the journals commonly publishing studies on geopolymer-based materials for heritage structures with Construction and Building Materials (21%), a Q1 journal based in the UK, has the highest publication.

Figure S11b displays the affiliation of authors by the number of publications, highlighting that most institutions are located in countries such as Italy with The most active institution is the University of Catania (24%). More detailed discussion about the countries, journal, and institution are found as supplementary information.

2.5. Active Authors

Table S4 summarizes the most active authors from 2013–2024, with Occhipinti, Roberta (10.5%), being the most active, with 4 articles on the development of geopolymers using pyroclastic deposits (i.e., pumice, volcanic ash, volcanic soil). More detailed discussion about the authors are found as supplementary information.

3. Geopolymers Used for Stone Architectural Heritage Structure Conservation

3.1. Definition and Formation Mechanism

Geopolymers are widely considered green alternative cementitious materials because of their low carbon emissions, high chemical resistance, as well as good thermal properties and mechanical performance [62,63]. This alternative material is formed by mixing geological (e.g., metakaolin, clays or volcanic ash) or industrial by-products/wastes (e.g., coal fly ash, palm oil fuel ash, silica fume, mine tailings, and slags) rich in alumino-silicate bearing phases as "precursors" with alkali hydroxides (e.g., NaOH, KOH, and lime) and silicate solutions (e.g., Na_2SiO_3 and K_2SiO_3) as "activators" to form an amorphous to semi-crystalline structure with tetrahedral coordination of silica and alumina covalently bonded to oxygen similar to the 3D arrangement of zeolitic materials, but with the presence interstitial water and porous structure [64–67].

Figure 12 shows a simplified schematic illustration of geopolymerization, a process composed of three steps: (i) dissolution, (ii) condensation, and (iii) hardening. The dissolution step involves

 doi:10.20944/preprints202603.0062.v1

breaking the aluminosilicate bonds of precursor materials into aluminate and silicate species under alkaline conditions, while the alkali ions (Na^+, K^+, and Ca^{2+}) neutralize the negative charge on alumina and silica monomers. This is then followed by condensation or coagulation-polymerization involving the formation of a geopolymeric matrix composed of monomers of sialate bonds (Si-O-Al) and siloxo bonds (Si-O-Si), and polymerization to form polysialate (-Si-O-Al-O-), poly(sialate-siloxo) (-Si-O-Al-O-Si-O-), poly(sialatedisiloxo) (-Si-O-Al-Si-O-Si-O), ferro-sialate (-Fe-Si-O-Al-O-), and aluminophospho (-Al-O-P-O) bonds [46,47]. Finally, the matrix hardens to form an amorphous to semi-crystalline 3D gel structure similar to zeolite and water [45,46].

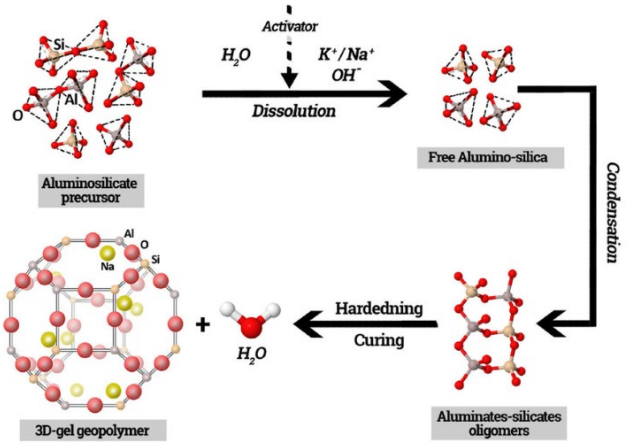

Figure 12. A schematic process diagram of geopolymerization (Reprinted with permission from Mabroum et al. [67], published by Elsevier, 2020).

3.2. Metakaolin-Based Geopolymers

Metakaolin (MK), produced by calcining of kaolinite at temperatures between 700−800 °C for 2-4 hours, is the most commonly used precursor for geopolymers, with chemical composition typically around 50−67% SiO_2, 31−42% Al_2O_3, 0.3−2% Fe_2O_3, 0.3−1.3% K_2O+Na_2O, 0.2−1.0% CaO+MgO, and 0.2−2.2% TiO_2 with an SiO_2/Al_2O_3 ratio of 1−2. Table 5 shows that 27 of the 34 studies used metakaolin as the precursor; that is, 12 papers used it as the main precursor, while the remaining 15 used it as an admixture. Allali et al. [68], for example, developed an MK-mortar to substitute $CaCO_3$ and $Ca(OH)_2$ as alternatives to traditional lime- and cement-based mortar in Moroccan heritage masonry to prevent salt efflorescence and improve flexibility. The MK-mortar achieved a 7-day compressive strength of 77 MPa using sodium silicate and sodium hydroxide as activators, with the addition of calcitic sand ($CaCO_3$) containing quartz, dolomite, and muscovite at a lime substitution rate of 47%. This approach is economically advantageous in Morocco because MK is cheaper and more widely available in comparison with slaked lime ($Ca(OH)_2$). Similarly, Clausi et al. [69] developed an MK-mortar with dolostone and sandstone as aggregates using the <0.5 mm particle fraction for dolostone and sandstone substrates. These authors formulated dense geopolymer with bulk densities of 2.7 and 3.0 g/cm3 and compressive strengths of 18 and 21 MPa, using dolostone and sandstone as aggregates, respectively. These dolostone and sandstone geopolymers resembled the original stones at a binder/aggregate ratio of 1 and a liquid-to-solid (L/S) ratio of 0.4, which could serve as replacements for natural dolostone and sandstone for restoration.

Meanwhile, Riccioti et al. [70] incorporated epoxy resin into the MK-slurry to improve its compressive strength, workability, and thixotropic behavior—a decrease in viscosity under constant stress/stirring and an increase when undisturbed—for application as fixing mortar on stone substrates for detached tuff-built AHB. These authors achieved higher compressive strength (49 MPa) than the control, a plain MK-geopolymer without epoxy resin (41 MPa), which can then be easily added with inorganic-colored pigments during restoration to match the original stone color. In addition, Moutinho et al. [72] developed a low compressive strength MK-based geopolymer (1−5

 doi:10.20944/preprints202603.0062.v1

MPa), which was achieved at high H_2O/Na_2O ratio (17 and 18) and formulated as adhesives for the repair of broken ancient ceramic tiles. The advantages of using MK-based geopolymer include (i) its good compressive strength even as the lone precursor material and (ii) its initial pale white color that can be easily modified by adding colored pigments to match the color of the original material to be repaired [76]. However, the main drawback of metakaolin is the need for thermal treatment by calcination before use to remove chemically bound water (OH groups) and convert naturally occurring kaolinite clay to metakaolin. Thus, its use is limited by supply and sustainability issues, unlike other precursors that can be recycled and repurposed (e.g., fly ash, blast furnace slag, sludge, and rice husk ash).

Table 5. Metakaolin-based geopolymer formulations and compressive strengths.

Country	Precursors SiO_2=50-67%, Al_2O_3=31-42%, Fe_2O_3=0.3-2% K_2O+Na_2O=0.3-1.3%, CaO+MgO=0.2-1.0% TiO_2=0.2-2.2%	Activators	Admixture	Aggregate	28-day compressive strength (MPa)	Ref.
Morrocco	Metakaolin	KS, KOH	Calcareous sand ($CaCO_3$)	–	16–41 (7d)	[68]
		SS, NaOH			63–77 (7d)	
		KS, KOH	$Ca(OH)_2$		7–10 (7d)	
		SS, NaOH			2–40 (7d)	
Italy	Metakaolin	SS, NaOH	-	Dolostone	18	[69]
				Sandstone	21	
				Quartz Sand	75	
Italy	Metakaolin	SS, NaOH	None	–	41	[70]
			Epoxy Resin		49	
Portugal	Metakaolin	SS, NaOH	Zeolite	–	4.6	[71]
		NaOH	Ca $(OH)_2$		1.0	
Portugal	Metakaolin	SS, NaOH	–	–	0.6–1.0	[72]
Czech Republic	Metakaolin	SS, NaOH	Waste Foam Glass	–	2.7–8.3	[73]
Czech Republic	Metakaolin (LO5)	KS, KOH	None	Quartz Sand	86.6	[74]
			Dolostone		72.7–87.7	
			Marble		73.8–75.7	
			Marlstone		78–80	
			Limestone		75–78	
			Feldspar		94–96	
Italy	Metakaolin	SS, NaOH	None	–	40	[75]
			Polyvinyl Acetate		38–42	
			Polydimethylsiloxane		37–42	
Italy	Metakaolin	SS, NaOH	Bromothymol Blue (Organic Dye)	–	–	[76]
			Phenolphthalein			
			Cresol red			
			Methyl orange			
Czech Republic	Metakaolin (LO5)	KS, KOH	Slag, Colored Pigments	Quartz sand		[77]
Czech Republic	Metakaolin (LO5)	KS, KOH	None	Quartz sand	75.5	[78]
China	Metakaolin,	SS, KS	Silica Fume	–	40–70	[79]

*Note: LO5: in house calcination of kaolinite; "SS": sodium silicate; "NaOH": sodium hydroxide; "KS": potassium silicate; "KOH": potassium hydroxide; "–": no data reported.

3.3. Fly Ash-Based Geopolymers

 doi:10.20944/preprints202603.0062.v1

Fly Ash (FA) is an industrial waste from coal fired power plants and biomass (e.g., wood, sugar cane bagasse, rice husk, tea dust and coconut shells) power plants, palm fuel oil industry, municipal waste incineration plants, and thermal power plant [64–66,114,115], and has been widely used as partial replacement to OPC for greener construction materials because of its pozzolanic properties. More recently, FA has become a popular precursor for geopolymers because of its high surface area and high alumina and amorphous silicate contents [80], as shown in Table 6.

Table 6. Summary of chemical and mineralogical composition of fly ash used in geopolymers.

Plant	Region, Country	SiO_2	Al_2O_3	Fe_2O_3	CaO	MgO	K_2O	TiO_2	Mineral Phases	Ref.
Neyveli thermal power plant	Tamil Nadu, India	52.2	25.8	3.6	3.0	2.2	0.6	1.3	Quartz (SiO_2), Calcite ($CaCO_3$), Hematite (Fe_2O_3)	[81]
Calaca Coal-fired power plant	Batangas, Philippines	79.3	–	4.0	5.6	4.4	1.6	0.08	Anorthite ($CaAl_2Si_2O_8$), Quartz (SiO_2), Goethite (α-FeOOH), Mullite ($3Al_2O_3{\cdot}2SiO_2$)	[82]
CFBC, coal-fired power plant	Philippines	27.4	23.2	21.7	16.5	6.2	0.9	0.9	Quartz (SiO_2), Calcite ($CaCO_3$), Magnetite (Fe_3O_4), Hematite (Fe_2O_3), Maghemite (γ-Fe_2O_3), Illite, Biotite	[118,119]
–	Italy	37.3	16.1	30.8	6.13	–	5.28	–	–	[83]
–	Italy	59.5	27.3	2.9	1.8	–	2.7	0.6	–	[84]

*Note:"–": no data reported, "CFBC": circulating fluidized bed combustion.

Table 7 lists 5 studies that employed FA, of which 4 used it as the main precursor material. Previous studies have shown that FA is generally blended with other precursors (e.g., MK and slag) to increase the compressive strength of the resulting geopolymer. For example, Kakria et al. [81] repurposed non-metallic fraction (NMF), a by-product from separating metallic and non-metallic components of printed circuit board (PCB) from sorting, and achieved a 28-day compressive strength of 27–29 MPa, from a mixture of 85wt% FA, and 15wt% NMF in comparison to 55wt% FA, 30 wt% MK, and 15 wt% NMF at 33–35 MPa with a binder/aggregate ratio of 0.33. Similarly, Dollente et al. [82] used FA mixed with silica fume, fiber, and fine aggregates as a restoration mortar for unreinforced historical masonry (URM), thereby increasing its tensile strength and improving its seismic competency. Out of the five (5) different types of fibers (i.e., polyvinyl alcohol (PVA), polypropylene (PP), stainless steel (SS), chopped basalt (CB), and carbon fibers (CF)) used in this previous work, PVA provided the highest increase in split tensile strength of 2.2 MPa in comparison to without fiber addition (1.6 MPa), while maintaining the compressive strength to around 12 MPa. Restoration of historical masonry was also reported by Longo et al. [83], who used FA with 5% MK and expanded glass aggregate as an inorganic matrix to create a fiber-reinforced cementitious material (FRCM), a composite composed of fiber mesh and mortar matrix, serving as reinforced plaster for historical masonry. This composite has a compressive strength of 6.0 MPa and a density of 1.03 g/cm^3, with a lower thermal conductivity of 0.9 W/m^{-2}K^{-1} compared with the traditional natural hydraulic lime (NHL)-based matrix at 1.1 W/m^{-2}K^{-1} in tuff-built masonry. The advantages of using FA include its valorization, pozzolanic properties, and its initially cement-gray color, which is quite helpful as a restoration material; thus, it is commonly used as a partial replacement for cement. To attain the desired strength, however, admixtures and careful adjustments of the concentrations of activators are required.

Table 7. Formulation of Fly ash-based geopolymers and compressive strength.

 doi:10.20944/preprints202603.0062.v1

Country	Precursors	Activators	Admixture	Aggregate	28-day compressive strength (MPa)	Ref.
Italy	Fly ash	SS, NaOH	Metakaolin, Printed circuit board (nonmetallic)	Sand	15.0–35.0	[81]
Philippines	Fly ash	SS, NaOH	Silica fume	Fine aggregate	12.6	[82]
Italy	Fly ash	SS, NaOH	Metakaolin,	Expanded glass	6.0	[83]
Italy	Fly ash	SS, NaOH	Metakaolin,	Expanded waste glass	7–10	[84]

Note: "SS": sodium silicate; "NaOH": sodium hydroxide; "KS": potassium silicate; "KOH": potassium hydroxide; "–": no data.

3.4. Slag-Based Geopolymers

Slag, a byproduct of the steelmaking industry, is generated when reducing and slagging agents (i.e., coke and limestone) are added to the iron ore to remove impurities. It is currently used as an alternative to Portland cement to develop sustainable construction materials, which are typically composed of 32.5–35.7% SiO_2, 9.94–11.6% Al_2O_3, 32.4–42.1% CaO, and 7–9.3% MgO. Table 8 summarizes 4 studies that used slag as the primary precursor and 1 article that used this material as an admixture. For example, Taburini et al. [85] developed a durable restoration mortar to strengthen ancient masonries by blending slag with other precursors (i.e., MK, wollastonite and sand) and achieved a 28-day compressive strength of 34.5 MPa, utilizing MK/slag/aggregate ratio of 1/2/3.5 with 63% of aggregate as sand and 37% as wollastonite fiber (composed of SiO_2 = 46.5%, Al_2O_3 = 0.96%, CaO = 42.1%, Na_2O = 0.15%, K_2O = 0.47%, MgO = 7.23%). Similarly, Maras et al. [86] achieved a comparable 28-day compressive strength of 33 MPa in a mixture of slag with the addition of slaked lime ($Ca(OH)_2$) at 5 wt%, and brick powders (0–2mm) with 8 M NaOH, as restoration material for Turkish Heritage structures. Notable results were also reported by Gupta et al. [87], who produced colored geopolymers by utilizing colored stone processing waste and slag, mixed at a 1:1 ratio, and hydraulically pressed. These authors reported pink, yellow, and white geopolymers with compressive strengths ranging from 15 to 25 MPa. Meanwhile, Kutlusoy et al. [88] used similar precursor materials as Maras et al. [86], but with higher amounts of slaked lime at 48% of precursors (slag/brick powders/slaked lime) and addition of sodium silicate and sand to be used as joint mortar for heritage masonry with a 28-day compressive strength of 30.6 MPa. These results suggest that slag-based geopolymers high in lime (CaO) exhibit better mechanical properties, reaching a compressive strength of at least 30 MPa after geopolymerization, which could be attributed to the dense formation of calcium-alumino-silicate-hydrate (CASH) and calcium-silicate-hydrate (CSH), similar to products found in hardened Portland cements. Slag is waste collected from blast furnaces in the steel industry and can be used for repair due to its cement-like properties: it hydrates readily and provides relatively high compressive strength.

Table 8. Formulations of slag-based geopolymers for heritage conservation and their compressive strength.

Country	Precursors SiO_2 =32.5-35.7%, Al_2O_3=9.94-11.6%, Fe_2O_3=0.32-1.25% CaO=32.5-42.1, MgO=7-9.3%	Activators	Admixture	Aggregate	28-day Compressive (MPa)	Ref.
Italy	Slag	SS, NaOH	Metakaolin, Wollastonite	River Sand	34.5	[85]
Turkey	Slag	NaOH	$Ca(OH)_2$, waste brick powder	–	25–33	[86]
India	Slag	SS, NaOH,	Dholpur Stone	Sand	15	[87]

 doi:10.20944/preprints202603.0062.v1

			Jaiselmer Stone		24	
			Kota Stone		25	
			Makarana Stone		25	
Turkey	Slag	SS, NaOH	Slaked lime	River Sand	18.1–30.6	[88]
		NaOH	Brick powder		11.5–26.2	
		KOH			11.1–27.1	

Note: "SS": sodium silicate; "NaOH": sodium hydroxide; "KS": potassium silicate; "KOH": potassium hydroxide; "–": no data.

3.5. Pyroclastic Material-Based Geopolymers

Table 9 lists 5 studies that utilized volcanic ash (VA) as a precursor for geopolymerization, collected from a single location in a village on the eastern flank of Mt. Etna, Italy, during the volcanic eruption in 2013. This material is composed of amorphous phases attributed to the presence of volcanic glass >60 wt% and phases of plagioclase ($(Ca,Na)Al_2Si_2O_8$), augite ($Ca(Mg,Fe)Si_2O_6$), forsterite ($Mg_2(SiO_4)$), and Fe/Ti-oxides, with a lime (CaO) content of 10.5 and Si/Al>2. For example, Finocchiaro et al. [89] achieved a 21-day compressive strength of 71 MPa by mixing VA with 20 wt% of MK with potassium-based activators (potassium silicate and potassium hydroxide), while Na-activators (sodium silicate and sodium hydroxide) only achieved a lower compressive strength of 51 MPa. Meanwhile, Occhipinti et al. [90] only achieved a 28-day compressive strength of 45 MPa, with VA and 20 wt% MK with Na-activators, which decreased to 39 MPa after adding VA aggregates (0.075-2mm). Similarly, Finocchiaro et al. [91] achieved a 28-day compressive strength of 25 MPa using Na-activators containing 80 wt% VA and 20 wt% MK, which increased to 34 MPa upon incorporation of 2% slaked lime.

Another alumino-silicate-rich geological material promising for geopolymer applications is volcanic soil. Volcanic soils (VS) are formed by the weathering of pyroclastic materials, such as lava, ash, and rock, and the accumulation of organic matter [120,121]. Table 8 shows a total of 4 studies that utilized of volcanic paleosoil (Ghiara) collected from the south slope Quarry of Mt. Etna, with a yellow-reddish color tone, amorphous with phases of anorthite, forsterite, hematite, augite, corundum and magnetite with Si/Al>2, and, was repurposed to be used as restoration material in historical building in Mt. Etna areas. For example, Finocchiaro et al. [89] achieved a 21-day UCS of 89 MPa by blending 20 wt% of MK into K-solution, compared with 51 MPa using Na-solution. Meanwhile, Occhipinti et al. [90,92] only achieved a 28-day UCS of 25 MPa using a Na-solution, but with the addition of volcanic paleosoil aggregates, it resulted in a lower strength value of 21 MPa.

Meanwhile, pumice—a silica-rich geological material formed when a silica-rich magma rapidly cools, releasing gases that form visible vesicles—from Aeolian Island, Sicily, Italy, was used by Occhipinti et al. [94]. This volcanic rock had a pale gray tone, was highly amorphous, and contained phases of corundum and plagioclase, with a high SiO_2 content (70%) and $SiO_2/Al_2O_3 > 5$. It was used as a precursor to restore building materials in Baroque Architecture in Sicily, originally built from Sicilian limestone. The pumice-based mortar developed in this work achieved a 28-day compressive strength of 12.7 MPa, with addition of 30 wt% MK, activated with sodium silicate (Na_2SiO_3)/sodium hydroxide (NaOH) ratio of 1.19, and L/S of 0.61 with comparable strength to western Sicilian limestones with compressive strength ranging from 0.5-20 MPa, and the geopolymer is classified as lower modulus ratio classified using Miller diagram, in comparison with Sicilian limestone, which according to the author an ideal restoration material for a less rigid material than original to avoid induced stress.

Table 9. Formulations and mechanical properties of pyroclastic-based geopolymer mortars.

 doi:10.20944/preprints202603.0062.v1

Country	Precursors In Molar Ratio: VA: Si/Al=2.5 VS: Si/Al=2.2 PM:Si/Al=3.1	Activators	Admixture	Aggregate	28-day compressive strength (MPa)	Ref.
Italy	Volcanic ash	SS, NaOH	Metakaolin		18–50 (21d)	[89]
	Volcanic soil				17–51 (21 d)	
	Volcanic ash	KOH, KS			29–71 (21 d)	
	Volcanic soil				30–89 (21 d)	
Italy	Volcanic ash	SS, NaOH	Metakaolin	Volcanic rock	39	[90]
				None	45	
	Volcanic soil			Volcanic soil	21	
				None	25	
Italy	Volcanic ash,	SS, NaOH	Metakaolin, $Ca(OH)_2$	None	34	[91]
			Metakaolin		25	
Italy	Volcanic ash	SS, NaOH	Metakaolin	None	45	[92]
				Volcanic rock	39	
	Volcanic soil			None	25	
				Volcanic soil	21	
Italy	Volcanic ash, Volcanic soil, Pumice	SS, NaOH	Metakaolin, Aluminum Powder	–	–	[93]
					–	
					–	
Italy	Pumice	SS, NaOH	Metakaolin,		7.2–12.7	[94]

Note: "SS": sodium silicate; "NaOH" : sodium hydroxide; "KS": potassium silicate; "KOH": potassium hydroxide; "VA": volcanic ash; "VS": volcanic soil; "–": no data.

3.6. Ceramic Waste-Based Geopolymers

Table 10 summarizes 5 studies that used ceramic waste as precursors for geopolymer production. This waste has a similar chemical and mineralogical composition to MK, thus showing potential as an MK substitute. Ceramic wastes are typically composed of 57% SiO_2, 33% Al_2O_3, 3.5% Fe_2O_3, 1.4% K_2O, 0.8% Na_2O, 0.8% CaO, with quartz (SiO_2), mica ($KAl_2(AlSi_3O_{10})(F,OH)_2$), feldspar $(K,N,Ca)(Al,Si)_4O_8$, and hematite (Fe_2O_3) as their major mineral components [110]. Several ceramic wastes, such as porcelain stone wares, raw pressed tiles, and bricks, or mixed ceramic waste, are incorporated with MK for geopolymer application. For example, Ricciotti et al. [95] utilized wastes from porcelain stoneware and ceramic tiles manufactured in Vicenza, Italy, and achieved promising results of using calcined raw pressed ceramic waste at 750 °C for 5 hours, and blending with MK at 11.6 wt%, achieving compressive strength of 41 MPa, while porcelain waste achieved 30 MPa, and mixed ceramic waste had 38 MPa. These authors conducted a preliminary investigation for conservation and restoration, wherein the slurry had good workability, making it easy to spread and model in tuff substrate as a fixing paste, while noting its ease in producing a colored product with the addition of water-based pigment, resulting in various types of colored MK-geopolymer. Fuggazzotto et al. [96–98] are prominent for using tile waste to develop a brownish-red geopolymer product. For example, Fuggazzoto et al. [96] blended tiles waste with MK and hydraulic lime at small amounts to promote binding, resulting to compressive strength of 14.3 MPa cured at room temp in comparison to curing 24h at 65 °C resulting to 9.79 MPa, attributed to crystallization of crypto-efflorescence inhibiting the gel formation at higher temperature, lowering its compactness and resistance, which coincided with the results in the increase of effective porosity, showing its promising result in ambient application Therefore, in their recent case studies these authors develop reintegration mortar to apply on-site on the deteriorated brick masonry of the Roman Odéon at Catania, due to its similar color tones to the brick elements. The test mortar was formulated using (i) tile waste or (ii) brick waste with MK and lime, and blended with aggregates such as carbonate sand, volcanic aggregates, and marble powder, depending on in-situ availability, color, and fineness. After application, the test mortar was monitored for 7 days and 28 days, and had good adhesion to

 doi:10.20944/preprints202603.0062.v1

substrate, negligible efflorescence, low shrinkage or less visible cracks, but brick waste formulation showed higher similarity to substrate in comparison to tile waste formulation, thus, it was not considered ethical due to intervention recognizability since during restoration the intervention material must still be recognizable. In another formulation by Fuggazzoto et al. [98], various aggregates, including carbonate sand, silica sand, and tile waste, were evaluated, achieving the highest compressive strength of 32 MPa with carbonate sand as the aggregate and mixing waste tiles with 20 wt% MK. In addition, Cappaso et al. [99] used brick waste blended with 20 wt% FA and achieved a compressive strength of 13.4 MPa, which is suitable as an alternative restoration mortar to traditional restoration materials such as lime mortar, OPC mortar, crushed bricks, sand, magnesian mortar, and natural limestone.

Table 10. Formulations and properties of ceramic waste-based geopolymers.

Country	Precursors SiO_2=57.3, Al_2O_3=32.7, Fe_2O_3=3.5, K_2O=1.4, Na_2O=0.78, CaO=0.83, with quartz, mica, feldspar, and hematite	Activators	Admixture	Aggregate	28-day compressive strength (MPa)	Ref.
Italy	Porcelain and stoneware waste, Raw pressed ceramic waste, Calcined Raw pressed ceramic, Gypsum Mixed	SS, NaOH	Metakaolin	–	30 25 41 4 38	[95]
Italy	Ceramic tile waste	SS, NaOH	Metakaolin, lime		3.5–14.3	[96]
Italy	Tile waste or Brick Wate	SS, NaOH	Metakaolin, lime	Carbonate sand, Volcanic aggregate, marble powder	– – –	[97]
Italy	Ceramic tile waste	SS, NaOH	Metakaolin	None Carbonate sand Silica sand Tile waste	14–27 18–32 6–7 6–16	[98]
Italy	Brick waste	SS, NaOH	Fly Ash None	Brick waste	13.4 5.3	[99]

Note: "SS" : sodium silicate; "NaOH": sodium hydroxide; "KS": potassium silicate; "KOH": potassium hydroxide; "–": no data.

3.7. Geopolymers Formulated from Other Materials

Table 11 lists one study that utilized tuff waste obtained from the natural stone processing industry. Capasso et al. [99] repurposed tuff waste consisting of a mixture of Neopolitan yellow tuff and Viterbo red tuff as restoration material for Italian heritage structures, and it was mixed with FA at 10 and 20 wt%, resulting in compressive strength of 1.48 and 1.34 MPa

A silica fume (SF)-based geopolymer was formulated by Baltazar et al. [100] as an alternative for traditional natural hydraulic lime (NHL) by mixing SF with superplasticizer to improve its fluidity, resulting in a compressive strength of 10-12 MPa, which was slightly lower in comparison to that without addition at 15 MPa.

Table 11 also summarizes a notable study by Beghoura et al. [101] that proposes repurposing tungsten mine tailings as a potential historical restoration material in Portugal. Mortar was formulated by blending mine waste, glass, MK, and Portland cement with expanded cork and was

 doi:10.20944/preprints202603.0062.v1

activated with sodium silicate (Na2SiO3) and sodium hydroxide (NaOH), resulting in a maximum compressive strength of 19.5 after 28 days. The application of aluminum powder and hydrogen peroxide as foaming agents also resulted in volume increases of 358% and 141%, respectively, providing a lightweight material for restoration.

Meanwhile, Rescic et al. [102] utilized Santena clay mixed with alkaline activators potassium hydroxide and potassium silicate that stabilized plasters for earthen based plaster of architectural heritage, which was then subjected to several durability tests like thermo-hygrometric cycle (an accelerated aging test for earthen material to assess durability caused by swelling) and shrinking test in a Climatic Chamber (heating first at 50 °C and 30% relative humidity for 6 hours and then cooling at 20 °C at 90% relative humidity for 6 hours, which is repeated 50 times). The results showed negligible weight loss of 0.30% for the stabilized plaster, identical to the original unstabilized plaster at 0.29%, indicating that the durability of the stabilized material was not significantly affected.

Table 11. Geopolymers formulated from wastes and local clays.

Country	Precursors	Activators	Admixture	Aggregate	28-day compressive strength (MPa)	Ref.
Italy	Tuff Waste (SiO_2=58.8%, Al_2O_3=31.82% Fe_2O_3=2.99% CaO=3.10% Na_2O=3.44% MgO=1.11% K_2O=9.34% TiO_2=0.53%)	SS, NaOH	Fly ash	Tuff waste	1.3–1.5	[99]
			None		0.8	
Portugal	Silica fume waste (SiO_2=97% Al_2O_3=0.15% Fe_2O_3=0.03% CaO=0.2% Na_2O=0.05% MgO=0.30% K_2O=0.80%)	SS, NaOH	Polycarboxylate-based superplasticizer	–	10–12	[100]
			None		14–15	
Portugal	Tungsten mine mud waste (SiO_2=46.7% Al_2O_3=17.0% Fe_2O_3=15.7% CaO=0.69% Na_2O=0.85% MgO=4.83%)	SS, NaOH	Portland cement, glass, metakaolin	Expanded Cork	10–19.5	[101]
Italy	Santena Clay (Smectite-Montmorillonite, Kaolinite, Illite, quartz, feldspars)	KOH, KS	–	–	Not conducted	[102]

Note: "SS": sodium silicate; "NaOH": sodium hydroxide; "KS": potassium silicate; "KOH": potassium hydroxide; "–": no data.

4. Compatibility Criteria in Using Geopolymers for Architectural Heritage Structure Conservation

According to the International Council on Monuments and Sites (ICOMOS, 2003), compatibility is critical for the structural conservation of AHSs; that is, the restoration (new) material and existing (old) material should have negligible negative impacts on the historical materials, especially in

 doi:10.20944/preprints202603.0062.v1

technical (chemical and mechanical), aesthetic, and historical (physical) aspects. In addition, Legislative Decree no. 42 of 22, 2004 of Ministry of Cultural Heritage and Activities (Ministero per i beni e le attività culturali, Rome) known as "Code of Cultural Heritage and Landscape defines restoration (in Art. 29, paragraph 4) as "the direct intervention on the property through a complex of operations aimed at the material integrity and recovery of the property itself at the protection and transmission of its cultural values" which also include structural upgrading in property at risk of earthquakes [111]. Meanwhile, in Philippines, Republic Act No. 10066 (National Cultural Heritage Act of 2009) defines restoration as "the action taken or the technical intervention to correct deterioration and alterations" [112]. This section provides an overview of the compatibility criteria used for geopolymers applied in the restoration and conservation of heritage structures, which are categorized in terms of (i) aesthetic, (ii) chemical, (iii) physical, and (iv) mechanical compatibility.

4.1. Aesthetic Compatibility

The aesthetic compatibility criteria govern the visual appearance of structures, which is primarily perceived by the naked eye to determine the similarity between the intervention and the original material in terms of color, efflorescence formation, and texture.

4.1.1. Color

To maintain the aesthetic appearance of the geopolymer to the original material, colorimetric analysis is conducted to assess the similarity of geopolymers with original materials. Color analysis is conducted using a spectrophotometer with a spot diameter of around 6 mm, measured at least six (6) times on different areas of the material, and reported in terms of CIELab (a color coordinate space developed by Commission Internationale de l'Éclairage in 1976 to describe the color visible to the naked eye). The CIELab provides each chromatic coordinate—L*, a*, and b—to determine the color difference (ΔE), following the formula in Equation 1, where L* denotes the lightness and ranges from 0 (total absorption or black) to +100 (white), while a* and b* denotes the green/red and blue/yellow values, respectively, both ranging between -60 and 60. The value of ΔE indicates the color similarity between two objects, with ΔE = 3 defined as the perceptibility limit; that is, values of ΔE > 3 indicate color differences readily perceptible to the naked eye [94,102].

$$\Delta E = \sqrt{(L_{reference} - L_{new})^2 + (a_{reference} - a_{new})^2 + (b_{reference} - b_{new})^2} \quad (1)$$

Table 12 lists the colorimetric analytical results reported in recent studies to assess c For example, Clausi et al. [69] determined the chromatic difference between original stones (i.e., sandstone and dolostone) and the metakaolin-based geopolymer binder with ornamental stone aggregates (i.e., sandstone and dolostone), yielding ΔE values of 5 and 11 for dolostone and sandstone, respectively. These authors attributed the high value to changes in the degree of lightness of sandstone at ΔL = -10, resulting in a paler tone compared to natural sandstones, allowing similar but recognizable color differences after restoration. Similarly, Fugazzotto et al. [98] formulated ceramic tile-based geopolymers with the addition of either carbonate sand, siliceous sand, ortile waste as aggregates,, and The ceramic tile-based geopolymer for Messana bricks, which were used during 2nd−3rd B.C. in the ancient urban city of Zancle-Messana, had the lowest observed ΔE of 6 using tile aggregates and 10 wt% MK, while the highest ΔE of 21 was obtained using silica sand and 20 wt% MK. Meanwhile, ceramic tile-based geopolymer for Gela Bricks, a reproduction of ancient bricks, achieves the lowest ΔE of 6.5 (10 wt% MK + silica sand) and 13 (10 wt% MK + tile waste), attributed to the different types of aggregate. In addition, Fugazzotto et al. [97] conducted a case study for in-situ application using tile-waste-based and brick-waste geopolymers as restoration mortars for the brick walls of Roman Odéon of Catania (2nd century A.D.), and after 3 months of monitoring, although no color difference (ΔE) was measured, a general visual comparison was conducted, indicating an indistinguishable color difference using brick waste geopolymer than tile waste geopolymer as restoration mortar for ancient brick walls.

Meanwhile, some studies conducted colorimetric analysis to obtain different pseudo-colors for each formulation, compared with raw pumice, due to its original whitish color, which can be easily

 doi:10.20944/preprints202603.0062.v1

adjusted to match the color of Sicilian limestones in UNESCO-listed Sicilian baroque cities. For example, Occhipinti et al. [94] evaluated the pseudo-colors of each pumice-based geopolymer mortar formulation and achieved the best ΔE values of 1.3 (20% MK) and 3.2 (30% MK), compared with the original pumice, highlighting the significant effects of precursors on the resulting color. Similarly, Fugazzotto et al. [98] evaluated the pseudo-colors of formulations containing different types of aggregates (i.e., carbonate sand and ceramic tiles) compared with the original ceramic tile waste. These authors reported ΔE of 1.5 using tile aggregates with 20 wt% MK and a high Na_2SiO_3/NaOH ratio of 2.3, suggesting that high amounts of Na_2SiO_3 in the mixture had a strong effect on the final color. The results of Fugazzotto et al. [98] were consistent with those of Occhipinti et al. [94], who reported that increasing Na_2SiO_3/NaOH from 0.33 to 2.67 decreased the ΔE values from 6.4 to 2.3, respectively, leading to a higher yellow component. Unfortunately, Rescic et al. [102] evaluated the color difference between the original raw clay and the geopolymer plaster for stabilizing earthen cultural heritage, resulting in a ΔE of 11.1 (prominent darkening, negative ΔL), but after subjecting it to thermo-hygrometric cycles, the ΔE decreased to 2.09.

Furthermore, colorimetric analysis has been conducted to determine color changes in geopolymers after exposure to environmental factors. For example, Occhipinti et al. [90] evaluated the color changes of VA- and VS-based geopolymer with or without 6 months of outdoor exposure, resulting in insignificant color changes (ΔE = 1.9–2.5) for VA-based geopolymers but with noticeable color differences for VS-based geopolymers (ΔE = 6.2–7.1). Similarly, Rescic et al. [102] mixed earthen Santena clay material with K_2SiO_3 and KOH for stabilization of earthen materials, resulting in ΔE of 2.09 after subjecting the stabilized earthen materials to accelerated weathering via thermohydrometric cycle tests.

Several authors also developed colored geopolymers to achieve the desired product color using various methods. For example, Perná et al. [77] applied an in-situ application protocol using inorganic pigments to match the original color of ceramic tiles during the renovation of churches in the Czech Republic. Similarly, Angelo et al. [76] developed a colored MK-based geopolymer using organic dyes (e.g., Bromothymol blue, phenolphthalein, cresol red, methyl orange), resulting in a blue, purple, violet, and brown-colored geopolymer. Meanwhile, Gupta et al. [87] developed a colored brick by adding colored waste stone powder from stone processing industries, resulting in pink, light yellow, and white colored geopolymer.

Table 13. Colorimetric analytical results of geopolymer mortars.

Binder Composition	Alkali Activator Ratio (NS/ NaOH)	Aggregates	Reference Color (L_{ref})	Color Difference (ΔE)	Change in Color Coordinate			Ref.
					ΔL	Δa	Δb	
MK	In molar ratio	Dolostone	Dolostone	4.7	-1.1	1.1	4.4	[69]
		Sandstone	Sandstone	10.9	-10.8	-0.52	1.6	
Tile+10 wt% MK	1	SS	Messina Bricks (Ancient Brick)	19	n.v.	n.v.	n.v.	[97]
		CS		9				
		CER		6				
Tile+20 wt% MK	1	SS		21				
		CS		12				
		CER		14				
Tile+20 wt% MK	2.3	SS		n.v.				
		CS		12				
		CER		18				
Tile+10 wt% MK	1	SS	Gela Bricks (Modern Brick)	6.5				
		CS		12				
		CER		13				
Tile+20 wt% MK	1	SS		8.5				
		CS		8.3				
		CER		10				

 doi:10.20944/preprints202603.0062.v1

Tile+ 20 wt% MK	2.3	SS CS CER		n.v. 7 8				
Tile+10 wt% MK Brick+10 wt% MK	1	CS	Odéon Bricks (Ancient Brick)	Recognizable Very Similar		n.v.		[98]
Pumice+20 wt% MK	1.33	None	Raw Pumice	1.3	0.5	0.25	1.16	[94]
Pumice+30 wt% MK	1.19			3.2	-2.9	0.24	1.2	
Santena Clay	1 (KS/ KOH)	None	Raw Clay	11.09	-9.49	-2.16	–5.32	[102]
Tile+10 wt% MK	1	SS CS CER	Raw Ceramic Tile	12 4 6		n.v		[98]
Tile+20 wt% MK	1	SS CS CER		3.2 9.2 9.5		n.v.		
Tile+20 wt% MK	2.3	SS CS CER		n.v. 5 1.5				
VA+ 20 wt% MK	n.v.	None VA	Prior to Weathering	1.87 2.49		n.v.		[94]
VS+20 wt% MK		None VS		7.10 6.19				
Santena Clay	1	None	Prior to Weathering	2.09	2.05	0.36	0.23	[102]

Note: “n.v.”: no value; “MK”: metakaolin; “SS”: silica sand; “CS”: carbonate sand; “CER”: tile waste; “VA” : volcanic ash; “VS”: volcanic soil; “NS”: sodium silicate; “NaOH”: sodium hydroxide; “KS”: potassium silicate; “KOH”: potassium hydroxide.

4.1.2. Presence of Efflorescence

The formation of efflorescence on AHS substrates not only deteriorates the durability of historic materials but also their aesthetic properties. Figure 13 illustrates a schematic diagram of how efflorescence forms in geopolymers, typically manifesting as white salt-like deposits on the surface or subsurface, gradually damaging the material. Recently, several authors monitored the presence of efflorescence; that is, the surface precipitation of white salt-like deposits composed of soluble sodium carbonates such as trona ($Na_3HCO_3 \cdot 2H_2O$), thermonatrite ($Na_2CO_3 \cdot H_2O$), natrite (Na_2CO_3), and natron ($Na2CO_3 \cdot 10H_2O$) on the surface of geopolymers, a process promoted by the movement of excess alkali activators through the porous network into the surface and then reacting with atmospheric CO_2 [45]. For example, Occhipinti et al. [90] evaluated the effects of atmospheric exposure for 6 months of VA- and VS-based geopolymers in Catania and found the presence of Trona ($Na_3H(CO_3) \cdot 2H_2O$), Natrite (Na_2CO_3), and Natron ($Na_2CO_3 \cdot 10H_2O$) on unexposed mortars, with Trona and Natron present on the surface and in bulk. Moreover, these authors reported the formation of Natrite (Na_2CO_3) covering 2/3 of the external surfaces for both VA-based mortar and binder, whereas for the VS-based geopolymers, only 1/4 of the external surface was covered in mortar and 1/5 in binder. The presence of natrite was attributed in this previous work to the leaching of natron and trona by rainwater, while natrite precipitated during dryer conditions. Similarly, Fuggazotto et al. [92] characterized the salt-like powdered deposits formed or scratching the surface of ceramic-based geopolymer by a scalpel, characterized them by X-ray Diffraction (XRD) and identified thermonatrite ($Na_2CO_3 \cdot H_2O$), and trona ($Na_3(CO_3)(HCO_3) \cdot 2H_2O$) in cured samples (65 °C for 24 hours) but not in samples cured under ambient conditions. Meanwhile, Clausi et al. [69] prevented the formation of efflorescence using aggregates rich with aluminum (sandstone) and calcium (dolostone). This was confirmed by the absence of new crystalline phases in XRD results after 90 days,

 doi:10.20944/preprints202603.0062.v1

including a reduction in FTIR bands around 1400 cm−1, related to the carbonate stretching vibration of Natron.

Other studies prevented the formation of efflorescence by subjecting the geopolymer paste to a desalination process involving a series of washes or baths to leach excess alkalis. For example, Geraldes et al. [103] investigated controlling salt efflorescence formation by monitoring the electrical conductivity (EC) of the baths using either NaOH or KOH as alkaline activators and drying at 21 °C and 40 °C. These authors reported the lowest EC was found when NaOH was used as the alkaline activator and drying in 40 °C, resulting to a electrical conductivity (σ) of 5000 μS/cm in a initial water bath consisting of 3.5 g of geopolymer paste in 50 g of distilled water in comparison to other formulation reaching approximately 8300 (NaOH at 21 °C), 9000 (NaOH at 21 °C) and 13,000 (KOH at 40 °C attributed to increased curing temperature, and smaller cation size of Na^+ easily leaching in the surface. After the 2nd and 3rd baths, the EC reached approximately 500 and 0 μS/cm (NaOH at 40 °C), and 1200 and 100 μS/cm (NaOH at 21 °C), respectively, indicating that soluble salts can be easily removed by immersion.

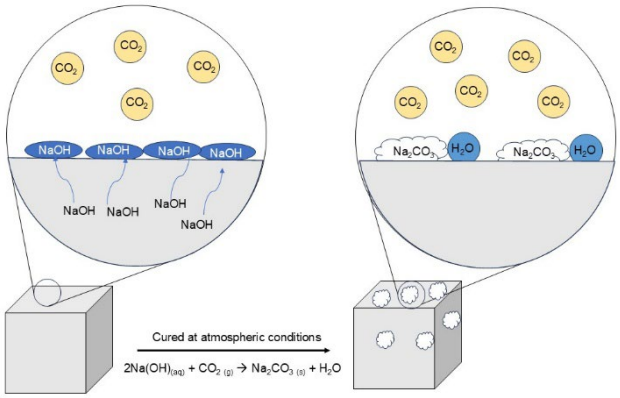

Figure 13. A schematic diagram of the formation of salt efflorescence [45].

4.1.3. Texture

The texture of the restoration material is important to maintain a surface texture similar to that of the original stone. This property is evaluated by macroscopic investigation and achieved by depending on the type, distribution, and sizes of aggregates used in the restoration mortar to mimic the original stone. For example, Clausi et al. [69] utilized natural stones as aggregates with a particle size distribution of less than 0.5 mm and a binder/aggregate ratio of 1:1. Similarly, Occhipinti et al. [94] incorporated natural volcanic rocks as aggregate at 30wt% of binders as restoration mortar with a size distribution at 32.5% (2< Ø < 1 mm); 31.5% (1.0 < Ø < 0.5 mm); 29% (0.5 < Ø < 0.125 mm); 6% (0.125 < Ø < 0.075 mm); 1% (Ø <0.075 mm), while Capasso et al.[99] incorporated tuff waste with an aggregate size of 0.3 to 4 mm at an aggregate/binder ratio of 0.5, but did not conduct a macroscopic investigation, as it focuses on repurposing materials, which is common for geopolymers due to their infancy towards application for AHS.

Unlike geopolymers as restoration mortars, other literature developed artificial stone mortars (ASM) with the distribution, type, and size of aggregates carefully designed to maintain similarity to stone; however, the drawback is their sustainability due to the use of Ordinary Portland Cement (OPC) as the binder. However, several results analyzed the difference in texture through microscopic [27,42] and macroscopic analysis [44] between original and new stone, assessing the texture (i.e., grains, phenocrysts, and matrix), but an on-site approach to achieve an antique appearance was scraping the mortar to expose the aggregates [98]. For example, Stefanidou et al. [44] designed an artificial stone to replicate an old marl limestone in the Archeological site of Pella, Greece; thus, recycling an old stone by crushing into 0-2mm, with addition of sand 0-2mm, 2-4mm, and dry soil, bound with cement, pre-casted, cured for 14 days, and grooved with a chisel to resemble the surface

 doi:10.20944/preprints202603.0062.v1

of original stone. Similarly, Menningen et al. [27] crushed the original tuff into fine and coarse aggregate ranging from 0-8mm, bound it with cement, colored it with an inorganic pigment to match the matrix color, and macroscopically compared it with the original tuffs. The results showed satisfactory results as the addition of natural stone maintains the fine-grained glassy matrix, mimicking the original volcanic tuff. Another notable challenge in synthesizing black tuffs is the difficulty of replicating the original color of the natural rock, as cement pastes tend to lighten during setting and hardening.

4.2. Chemical Compatibility

4.2.1. Microstructure

Figure 14 shows scanning electron microscopy (SEM) photomicrographs collected to evaluate the microstructural differences between the original substrate and the restoration mortar. Riccioti et al. [70,75,95], for example, observed through microstructural analysis a homogenous and continuous phase in the interface between the geopolymer and substrate (i.e., ceramic, tuff, and concrete) with no presence of microfractures and voids, indicating high chemical compatibility and good adhesion. Similarly, Fugazzotto et al. [98] conducted SEM analysis and found that the interface between the geopolymer and ancient brick substrates was well compatible, with no visible cracks or microcracks.

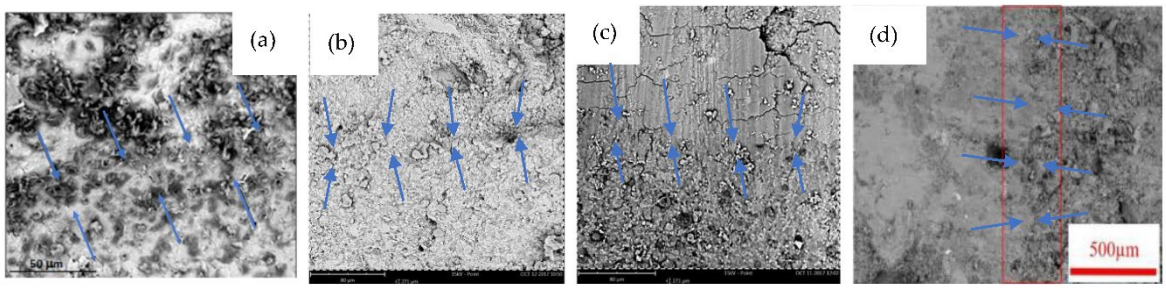

Figure 14. Interface transition zone between geopolymer and (a) ceramic, (b) tuff, (c) concrete, and (d) ancient bricks (Reprinted with permission from Ricciotti [70,75,95], MDPI, 2017, 2022, and Fugazzotto [97], Taylor & Francis, 2024.).

4.2.2. Ionic Release

Ionic Release is evaluated to measure the quantity of ionic species released from restoration mortars, to assess the potential formation of soluble salts that can further degrade the ancient stones. For example, Ricciotti et al. [70] evaluated the chemical compatibility by measuring the release of ionic species when in contact with water to determine the soluble salt content with respect to thickness, results showed trace concentrations of sodium ions (Na^+) after the 1st wash using ultrapure water at around 6.7 and 5.5 mg/g sample, for 3 mm and 6 mm thickness, respectively. Then, 2nd washing, the sodium ions (Na^+) decreased to 1.7 mg/g sample (3 mm) and 1.6 mg/g sample (6 mm), while 3rd washing resulted to 1.3 mg/g (3 mm) and 1.1 mg/g (6 mm), finally wash resulted to comparable ionic release of 0.7 mg/g (3 mm) and 0.7 mg/g sample (6 mm), while pH maintained at 10−11, thus indicating a comparable difference regardless of thickness of the sample.

4.3. Physical Compatibility

Table 13 summarizes the physical characteristics of restoration material, specifically on porosity, water absorption, capillary absorption, and density in comparison with the properties of the original substrates to determine the similarity based on the percent change. For example, Clausi et al. [69] produced a mortar with porosity and density (2.7−2.9 g/cm3) similar to those of natural stone, providing an alternative for substitution or as a repair mortar compatible with the original material. Similarly, Capasso et al. [99], reported a high similarity of open porosity capacity of tuff waste

 doi:10.20944/preprints202603.0062.v1

(39–42%) and brick waste (27–34%) geopolymer in comparison traditional mortars (30-40%) and limestones bioclastic limestone (24–30%), while also maintaining an similar water absorption through capillarity for tuff waste (20-33 mg/cm^2 s$^{-1/2}$) and brick waste (19-26 mg/cm^2 s$^{-1/2}$) geopolymers in comparison to traditional mortars at 28.5 mg/cm^2 s$^{-1/2}$ and natural bioclastic limestone at 31.3 mg/cm^2 s$^{-1/2}$ used in stone heritage and found high similarities in these properties between geopolymers and original materials. Meanwhile, Occhipinti et al. [94] reported the importance of a lightweight pumice-based geopolymer, with an average density of 1.4 g/cm3 and an open porosity of 35–37%, aimed at preventing additional stress on Western Sicilian limestone used in Sicilian AHS, with compressive strength ranging from 0.5–20 MPa during restoration. Meanwhile, Baltazar et al. [100] compared the open porosity and density of traditional lime-based grouts with geopolymer grouts and reported a lower density of approximately 1.35 g/m^3 for the former and 1.2 g/cm^3 for the latter. In contrast, open porosity was around 50% for lime-based grouts and 20–40% for geopolymer grouts.

Table 13. Physical properties of geopolymers in comparison with reference material.

Property	Geopolymer type	Geopolymer value	Reference material	Reference material value	Percent change (%)	Similarity	Ref.
Open Porosity (%)	Pumice+MK	36.5	Sicilian Limestone	–	–	–	[94]
	MK+dolostone	17.8	Dolostone	–	–	Similar (from author)	[69]
	MK+sandstone	14.1	Sandstone	2–6	57–85	High	
	FA	20-40	Natural Hydraulic Lime	50	20–60	Very High to High	[100]
	Tuff	39.4-42.3	Aerial Lime Mortar	25.9	52–63	High	[99]
			NHL	23.5	67–80	High	
			OPC	18.8	113–128	Medium	
			Repair Mortars	26.2	50–61	High	
			Historical Magnesian Mortar	30–40	6–31	Very High	
			Natural Limestone	24–30	39–40	Very High	
	Brick	26.2-34.2	Aerial Lime Mortar	25.9	1.1–23	Very High	
			NHL	23.5	11.5–45.5	Very High	
			OPC	18.8	39.4–81	Very High	
			Repair Mortars	26.2	0–31	Very High	
			Historical Magnesian Mortar	30–40	12.7–15	Very High	
			Natural Limestone	24–30	8.3–13	Vert High	
Water Absorption (%)	Tuff	26.7-30.97	n.d.	–	–	–	[99]
	Brick	15.71-19.75	n.d.	–	–	–	
Capillarity Absorption (mg/cm^2 s$^{-1/2}$)	Tuff	20.9-33.4	Aerial Lime Mortar	13.9	50–140	Medium to High	[99]
			NHL	9.40	122–225	Medium	
			OPC	3.4	514–882	Very Low	
			Repair Mortars	24.2	13.6–38.01	Very High	
			Historical Magnesian Mortar	28.5	17–27	Very High	
			Natural Limestone	31.3	6.7–33	Very high	
	Brick Based	19.5-26.6	Aerial Lime Mortar	13.9	40–91	High	
			NHL	9.40	107–183	Medium	
			OPC	3.4	473–682.3	Low	
			Repair Mortars	24.2	10–19	Very High	
			Historical Magnesian Mortar	28.5	6.6–31	Very High	
			Natural Limestone	31.3	15–37	Very High	
Bulk Density (g/cm^3)	MK+dolostone	2.8	Dolostone	2.7	3.7	Very High	[69]
	MK+sandstone	2.9	Sandstone	2.9	0	Very High	
	Pumice+MK	1.43-1.46	Silician Limestone	–	–		[94]
	Silica Fume	1.0-1.2	NHL	1.35	11–25	Very High	[100]

 doi:10.20944/preprints202603.0062.v1

Tuff	1.35-1.4	-	–	–	[99]
Brick	1.73-1.76	-	–	–	

Note: Similarity = Very High (0-50), High (50-100), Medium (100-300), Low (300-500), Very Low (>500).

4.4. Mechanical Compatibility

4.4.1. Adhesion

Baltazar et al. [100] developed a silica fume (SF)-based geopolymer mortar as grouting for historical masonry. To assess the adhesion strength—defined as the bond strength between the restoration material and the substrate—of silica fume mortar compared to traditional lime-based mortar, an adhesion test is typically conducted. The adhesion test is a quantitative method for measuring the bond strength between the restoration material (e.g., mortar, grout, adhesive) and the original substrate (e.g., stone, tiles, ceramics, bricks) by developing several hybrid specimens. Based on the study of Baltazar et al. [100], silica fume-based geopolymers had higher flexural strength (0.6–0.9 MPa) compared with traditional natural hydraulic lime grout (0.1 MPa), an increase of around 90% (Figure 15a). Meanwhile, Tamburini et al. [85] conducted a pull-off test on fiber-reinforced slag-MK geopolymer mortar on ancient and modern construction clay bricks and reported good adhesion (0.9-1.7 MPa) to the ancient bricks, with failures observed in the original substrate (Figure 15b). In comparison, failure in the geopolymer-modern bricks occurred at the reinforcement layer with slightly higher adhesion of around 1.2-2.81 MPa. Similarly, Fugazzotto et al. [97] conducted an adhesion test with a "sandwich" specimen (Figure 15c) using two ancient bricks and reported poor adhesion with sand aggregates and a ceramic-based geopolymer, attributed to fracture at the interface, but no quantitative values were presented.

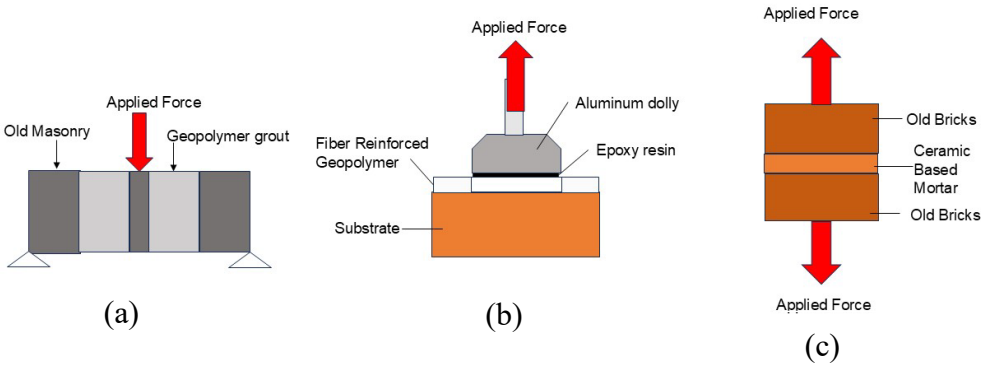

Figure 15. Different Adhesion Test conducted for a) grout from Baltazar et al. [100], b) plaster from Taburini et al. [85], and c) adhesive from Fugazzotto et al. [97].

4.4.2. Surface Hardness

Maras [86] conducted an in-situ Non-destructive technique (NDT) to evaluate the surface hardness of historical mortars and geopolymer mortars and reported a medium level of similarity based on the rebound hardness test. Also, Capasso et al. [99] conducted a surface hardness test using the Shore-D hardness test but did not compare the results to the original materials.

4.4.3. Compactness

Compactness is measured using ultrasonic pulse velocity (UPV), another in-situ NDT method to determine the degree of damage in the material, as it depends on the material's density and modulus of elasticity, which can result in a degree of deterioration. For example, Maras [86] evaluated the compactness of the material between geopolymer and original mortars and found a higher value for geopolymers, with an increase of 50% compared to the in-situ joint historical mortars.

 doi:10.20944/preprints202603.0062.v1

4.4.4. Compressive Strength

Occhipinti et al. [94] compared the mechanical properties of a pumice-based geopolymer and traditional limestone using Miller Diagrams and showed similarities to low-strength limestone. Meanwhile, Capasso et al. [99] compared tuff and brick waste geopolymer with conventional materials in cultural heritage, showing similarities to the original materials, with tuff waste geopolymer (0.81−1.34 MPa) and brick waste geopolymer (5.34−13.4 MPa) matching natural limestone (10.1 MPa). Similar to Baltazar et al. [100], who reported a higher compressive strength for silica-fumed-based geopolymer (10−15 MPa) than for traditional lime-based mortar (8 MPa). However, Dollente et al. [82] compared the compressive strength without addition (12.55 MPa) and with the addition of fibers (1.81−12.1 MPa), resulting in similar compressive strength depending on the type of fiber added to the mixture.

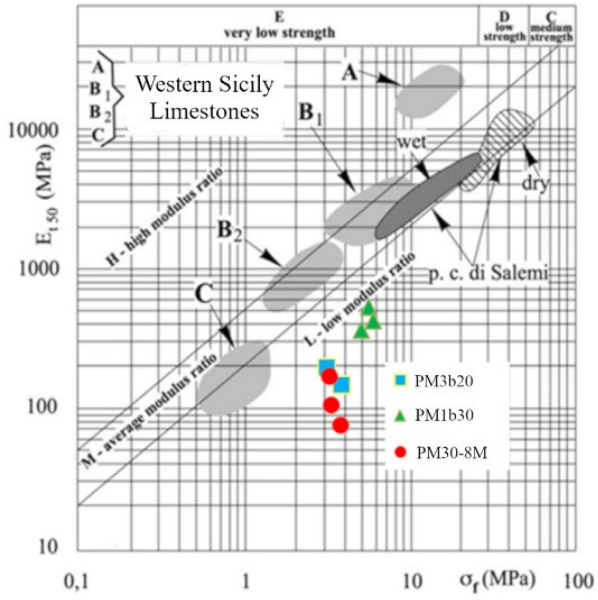

Figure 15. Deer-Miller Diagram (Reprinted with permission from Occhipinti et al. [94], published by Elsevier, 2020) comparing the mechanical properties of geopolymers and natural stones in Sicily, Italy.

4.4.5. Tensile Strength

Dollente et al. [82] incorporated five (5) types of fibers (polyvinyl alcohol, chopped basalt, copper-coated stainless steel, polypropylene, and carbon fiber) into a fly ash-silica fume geopolymer mortar to enhance tensile strength while maintaining competent compressive strength, potentially improving the earthquake resistance of historical masonry. The results showed that the addition of PVA, stainless steel, and chopped basalt fibers achieved a comparable compressive strength of 12.0, 12.1 MPa, and 9.9 MPa, respectively, from a 12.6 MPa control mortar, while the increase in tensile strength was 2.2, 1.64, and 1.8 MPa in comparison to 1.58 MPa of control mortar. Meanwhile, Tamburini et al. [85] developed a slag-MK geopolymer with river sand as aggregate and fibrous wollastonite as filler, resulting in 28-day compressive and tensile strengths of 34.5 MPa and 4.8 MPa, respectively, which was used as a mortar matrix for fiber/mesh-reinforced cementitious composites.

4.4.6. Flexural Strength

Flexural strength is defined as the ability of the material to resist bending under load, as measured by the stress prior to fracturing. The importance of determining the susceptibility to resist deformation and cracking, a similar property to original materials (i.e., traditional mortars or rocks). For example, Capasso et al. [99] compared the flexural strength of traditional tuff and brick waste stone-based geopolymers and showed a high degree of similarity for tuff waste-based geopolymer,

 doi:10.20944/preprints202603.0062.v1

while brick waste-based geopolymer showed low to high similarity to traditional mortars. Meanwhile, silica fume-based grout of Baltazar et al. [100] was higher strength at 1.0-1.5 MPa than traditional natural hydraulic lime (NHL) mortars at 0.2 MPa, attributed to the reaction of silica fume in alkali activators to form an aluminosilicate gel in the microstructure. Similarly, Clausi et al. [69] obtained MK-geopolymers that had the highest flexural strength of 3.2-3.6, but did not conduct a comparison between the original stones (i.e., dolostone and sandstone).

Table 14. Mechanical properties of geopolymer in comparison with reference materials.

Property	Geopolymer type	Geopolymer	Reference	Ref. material value	Percent Change%	Similarity	Ref.
Adhesion (MPa)	Silica fume	0.6–0.9	NHL	0.1	500–800	Very Low	[100]
	Slag	0.89–1.65	SM Bricks (substrate 1)	–	–	–	[85]
	Slag	1.21–2.81	EM Bricks (substrate 2)	–	–	–	
Surface Hardness	Slag	31–39	Historical Mortars	10–20	95–210	Medium	[86]
	Tuff	26.5–53	In-situ Mortar	–	–	–	[99]
	Brick	31.2–75.8	In-situ Mortar	–	–	–	
Compactness (m/s)	Slag	3000–4000	In-situ Mortar	2000-3000 m/s	50	Very High	[86]
Compressive (MPa)	Pumice	3–6 MPa	Type A WSL	8–20 MPa	62–70	High	[94]
			Type B_1 WSL	3–10 MPa	0–40	Very High	
			Type B_2 WSL	1–3 MPa	0–200	Very High to Medium	
			Type C WSL	0.5–1.5 MPa	100–1100	Medium to Very Low	
	Silica Fume	10–16	NHL	9 MPa	11–77	High to Very High	[100]
	Tuff	0.81-1.48	Aerial Lime Mortar	0.5	62–196	Medium to High	[99]
			NHL	3.7	78–60	High	
			OPC	24.8	94–96	High	
			Repair Mortars	3.5	57–77	High	
			Historical Magnesian Mortar	–	–	–	
			Natural Limestone	10.1	85–92	High	
	Brick	5.3–13.4	Aerial Lime Mortar	0.5	960–2580	Very Low	
			NHL	3.7	43–262	Medium to High	
			OPC	24.8	46–75	High to Very High	
			Repair Mortars	3.5	51–282	Medium to High	
			Historical Magnesian Mortar	–	–	–	
			Natural Limestone	10.1	47.5–32.7	Very High	
	MK	18	Dolostone	–		–	[69]
	MK	21	Sandstone	–		–	
	FA	1.8–12.1	Plain Mortar	12.5	0–86	High to Very High	[82]
Tensile (MPa)	FA	0.6–2.2	Plain Mortar	1.6	37.5–62.5	High to Very High	[85]
	Slag	4.8	None	n.d.	–	–	
Flexural (MPa)	Silica Fume	0.2	NHL	1.0–1.5	80–86	High	[100]
	Tuff	0.4–1.23	Aerial Lime Mortar	0.24	66–412	Medium to High	[99]
			NHL	1.00	23–60	Very High	
			OPC	4.70	74–91	High	
			Repair Mortars	–	–		
			Historical Magnesian Mortar	–	–		
			Natural Limestone	–	–		
	Brick	2.85–4.58	Aerial Lime Mortar	0.24	1087–1808	Very Low	
			NHL	1.00	185–358	Low to Medium	
			OPC	4.70	2–39	Very High	
			Repair Mortars	–	–	–	
			Historical Magnesian Mortar	–	–	–	
			Natural Limestone	–	–	–	
	MK	3.2	Dolostone	–	–	–	[69]
	MK	3.6	Sandstone	–	–	–	

 doi:10.20944/preprints202603.0062.v1

Note: WSL- Western Sicilian Limestone , NHL- Natural Hydraulic Lime, OPC -Ordinary Portland Cement, "-": no data, Note: Similarity = Very High (0-50), High (50-100), Medium (100-300), Low (300-500), Very Low (>500).

5. Recent Applications of Geopolymers in Architectural Heritage Structure Conservation

Recent AHS conservation literature has commonly formulated geopolymer-based repair mortars to restore or patch degraded parts of the original stone substrate, followed by the application of consolidants to fill cracks and fix loosened material. In addition, masonry strengthening has been studied as a retrofitting technique to improve its resistance against seismic activity; however, the majority of these studies only presented potential for restoration and a preliminary on-site evaluation. A few studies have also reported the successful on-site application of the material, prioritizing ceramic tiles and bricks, while studies related to on-site application on natural rocks have been well reported. Table 15 shows the list of recent applications of geopolymers in cultural heritage, indicating the type of geopolymer, purpose, and original substrate.

5.1. Repair Mortars

Repair mortars are applied to the original material as an alternative to restoring large patches of degraded original material. For example, Allali et al. [68] developed an MK-based geopolymer with Ca-rich components (lime and calcareous sand) as additives to maintain chemical compatibility with traditional materials for Moroccan AHSs instead of traditional lime-based mortars and concrete, which easily form salts, dense, and low flexibility, which showed a 7-day compressive strength ranging from 16-77MPa,($CaCO_3$) and 2-40 MPa ($Ca(OH)_2$). Similarly, Maras [86] developed a slag-based geopolymer as repair mortar for Turkish AHSs because the use of traditional low-strength mortars resulted in visible cracks post-earthquake episodes, with a 7-day compressive strength of 10-20 MPa. Meanwhile, 28-day compressive strength of repair mortars for Italian AHSs using metakaolin and pumice-based resulted in 18-21 MPa and 7 to 12 MPa, respectively [69,94]. In addition, Kutlusoy et al. [88] aimed for a structurally competent masonry by utilizing a high-strength slag-based geopolymer with 7-day compressive strengths of 20.7 MPa to 36 MPa.

5.2. Consolidants

Meanwhile, consolidants are adhesives or grouts used to fill small gaps and cracks and to fix broken original ceramics and natural stones. For example, Moutinho et al. [71,72] used MK-based geopolymer as consolidants to fix broken ceramic tile, resulting to a 7-day compressive strength of 0.6MPa to 3 MPa, whereas Baltazar [100] utilized it as grout for old stones in historical masonry and resulted to a 28-day compressive strength of 10-12 MPa (with superplasticizer) and 14-15 MPa (control). Meanwhile, Riccioti et al. [70] applied an MK-based geopolymer with epoxy resin as a fixing paste for tuff and concrete substrates, resulting in a 28-day compressive strength of 40-50 MPa.

5.3. Masonry Strengthening

Furthermore, strengthening historical masonry with high-strength geopolymer mortars reinforced with fibers to withstand seismic vibration. For example, Dollente et al. [82] applied a FA-based geopolymer mortar with fiber addition to unreinforced historical masonry, resulting in tensile strengths of 0.6 MPa to 2.2 MPa, compared to the control of 1.6 MPa. Meanwhile, other studies aimed to provide seismic reinforcement for historical masonry. For example, Tamburini et al. [85] reported fiber-mesh-reinforced mortar, in which adhesion strength was measured by pull-out tests on the original substrate (clay bricks), resulting in 0.9 to 1.65 MPa in historic bricks and 0.9 MPa in the control, while 1.6 to 2.8 MPa in modern bricks and 2.7 MPa in the control. Similarly, Longo et al. [83] tested in coupons resulting in a tensile strength of 867.69 MPa

 doi:10.20944/preprints202603.0062.v1

5.4. Others

Finally, the remaining studies did not discuss applications for AHBs but showed potential for restoration through the development of colored geopolymers [76,87] without the addition of commercial-colored pigments. For example, Gupta et al. [87] formulated slag-based geopolymer bricks with the addition of colored-stone processing waste, resulting in pink, yellow, greyish, and white-colored bricks with a compressive strength of 15-25 MPa. Meanwhile, Angelo et al. [76] developed colored MK-based mortar by adsorbing Bromothymol blue, methyl orange, cresol red, and phenolphthalein, resulting in blue, yellow, violet, and purple geopolymer, respectively.

Another notable is the potential for restoration of the effect of maturation in different environments [78] in air, demineralized water, or seawater, using an MK-based geopolymer, resulting in 86.5 MPa, 79.3 MPa, and 87.2 MPa after 28 days of maturation. Meanwhile, MK-silica fume-based with [79] with sodium silicate (Na_2SiO_3) and potassium silicate(K_2SiO_3) resulted in a 7-day compressive strength of 30 to 58 MPa, while a MK-fly ash geopolymer with expanded waste glass aggregates resulted in a 48-day compressive strength of 10 MPa [106]

Recently, on-site applications in restoration have been slowly rising. For example, Fugazzotto et al. [97] applied a ceramic-based geopolymer mortar to ancient bricks as substrate, resulting in a similar chromatic difference. Similar to Perna [77], the application of geopolymers for fixing historical ceramic tiles and sandstones. However, further developments are needed for application to highly weathered ancient stones, in order to develop a sustainable material that enhances the long-term preservation of stone architectural heritage structures.

Table 15. Current application of geopolymers in architectural heritage structure conservation.

Country	Geopolymer	Purpose/Application	Original Materials	Architectural Heritage Structure	Ref
Morrocco	Metakaolin	Repair mortar	Lime-based mortar	Moroccan Historical Monument	[68]
Italy	Metakaolin	Repair mortar	Sandstone and dolostone	Not specified	[69]
Turkey	Slag	Repair mortars	Low strength mortars	Turkish Historical Masonry	[86]
Italy	Volcanic ash Volcanic soil	Repair mortars/binders	Not specified	Catania Architectures	[89]
Italy	Volcanic ash Volcanic soil	Repair mortars/binders	Not specified	Catania Architectures	[90]
Italy	Volcanic ash Volcanic soil	Repair mortars/binders	Not specified	Catania Architectures	[92]
Italy	Volcanic ash, Volcanic soil, Pumice	Repair mortars/binders	Not specified	Not specified	[93]
Italy	Volcanic ash,	Repair mortars	Mosaics	Cathedral of Monreale, Sicily	[91]
Italy	Pumice	Repair mortars	Sicilian limestones	Sicilian Baroque Cities	[94]
Italy	Tile waste or Brick waste	Repair mortars	Ancient bricks	Cathedral of Messina, Sicily, and Archeological Ruins in Gela, Caltanissetta	[97]
Italy	Ceramic tile waste	Repair mortar	Ancient bricks	Roman Odéon of Catania	[98]
Italy	Brick waste	Repair mortar	Limestone, lime mortars	Not specified	[99]
Italy	Tuff waste	Repair mortar	Limestone, lime-based mortars	Not specified	[99]
Portugal	Tungsten mine waste	Repair mortar	None	Not specified	[101]
Italy	Metakaolin	Consolidant	Tuff, concrete, ceramic	None	[70]
Portugal	Metakaolin	Consolidant	Ceramic tiles	None	[71]
Portugal	Metakaolin	Consolidant	Ceramic tiles	None	[72]
Italy	Metakaolin	Consolidant	Ceramic artworks	None	[75]
Czech Republic	Metakaolin (LO5)	Consolidant	Ceramic tiles	None	[77]
Italy	Porcelain stoneware Waste Raw pressed ceramic	Consolidant	Ceramic artworks	None	[95]

 doi:10.20944/preprints202603.0062.v1

Country	Geopolymer	Purpose/Application	Original Materials	Architectural Heritage Structure	Ref
	Calcined raw pressed ceramic				
	Gypsum				
	Mixed				
Portugal	Silica fume	Consolidant/Grout	Hydraulic lime	Non specified	[100]
Italy	Local clay	Consolidant/Plaster	Local clay	Earthen Architectures	[102]
Turkey	Slag	Strengthening historical masonry	Ceramic brick masonry	Turkish Historical Architectures	[90]
Italy	Fly ash	Strengthening historical masonry	Tuff and brick masonry	Not specified	[83]
Philippines	Fly Ash	Strengthening historical masonry	Unreinforced stone masonry	Not specified	[82]
Italy	Slag	Strengthening historical masonry	Ancient and modern brick masonry	Not specified	[85]
Czech Republic	Metakaolin	Valorization	None	None	[73]
Czech Republic	Metakaolin (LO5)	Valorization	None	None	[74]
Italy	Ceramic tile waste	Valorization	None	None	[96]
Italy	Fly ash	Valorization	None	None	[81]
Italy	Metakaolin	Colored geopolymer	None	None	[76]
India	Slag	Colored geopolymer	None	None	[87]
Czech Republic	Metakaolin (LO5)	Investigation of maturation environment	None	None	[78]
China	Metakaolin,	Investigation of modified activators (Na_2SiO_3 and K_2SiO_3)	None	None	[79]
Italy	Fly ash	Investigation of lightweight Aggregates	None	None	[106]

Note: “LO5” means in-house calcination of clay at 750 °C for 4-5 hours.

6. Case Study of Compatible Geopolymers for Heritage Structures in the Philippines

In the Philippines, there are two (2) natural rocks commonly used as building materials for AHS during the 16th to 19th century, which are currently considered as National Treasures. The first rock is “asohe” or “asoje”, a local term for volcanic tuff commonly used in the construction of the Walled City of Intramuros, Fort Santiago, in Manila, Historic City of Vigan, Baroque Churches in Central Luzon (e.g., Taal, Silang, Tanay, and Caloocan), and Albay (e.g., Tabaco and Daraga). The rock can be classified into three types. First is the pumice-cinder tuff, which resembles volcanic breccia and has a purple to brownish-gray color, with inclusions ranging from pebble- to cobble-sized rocks. Second is a fine-grained concretionary tuff, with a color varying from light gray to light brown and a fragment size range from fine sand to silt. The third type is in the presence of buff clay horizons exposed at the quarry site on the south bank of the Pasig River, with a fine-grained matrix ranging from fine silt to fine sand with dark-blue glassy fragments, round concentrical “mud balls”, and an abundance of pumice sizes ranging from 0.5-2 cm [107]. Meanwhile, the second rock is coral rock or coral stone, commonly used for the walls of Baroque Churches built during the Spanish Era in various islands and coastal regions in the Philippines. For example, the Island of Bohol has several baroque churches declared as tangible-immovable National Cultural Treasures (NCT), under the National Cultural Heritage Act of 2009, such as church in Loboc (1734), Maribojoc (1852–1872), Baclayon (1727), Loon (1864), Dimiao (1800s), Dauis (1697), Loay (1822), Cortes (1800s), Calape (1802), including Watchtowers (e.g., Maribojoc, Dauis, Panglao, Baclayon, Loay and Balilihan) and Residential Houses (Casa Rocha, Tagbilaran) [122,123]. Figure 16 shows the geology of the Philippines, including the location of AHS, built from tuff and coral rock.

 doi:10.20944/preprints202603.0062.v1

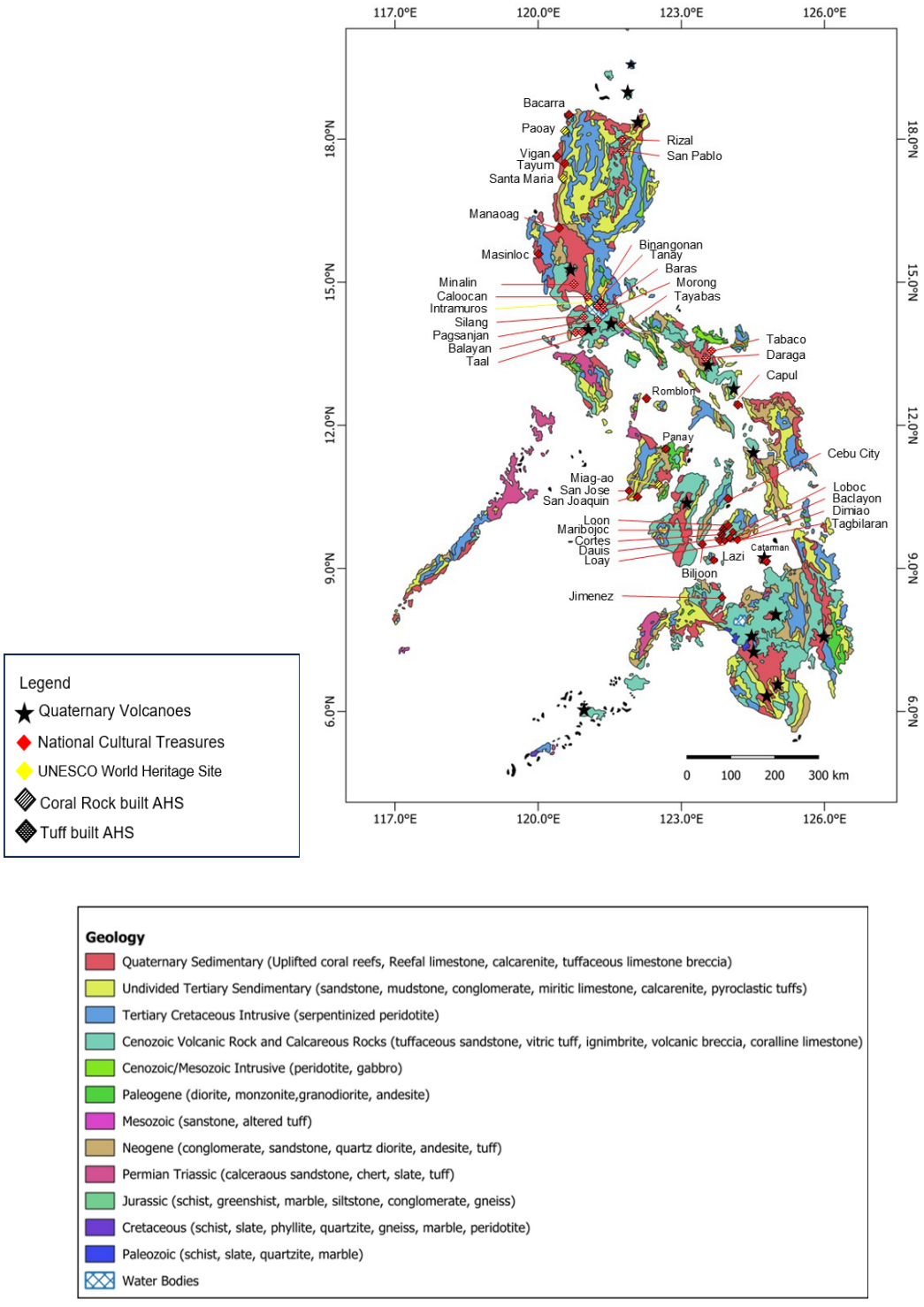

Figure 16. Geological map of the Philippines and locations of notable AHS built from tuff and coral rockA brief, critical analysis was conducted to propose a suitable geopolymer as an alternative conservation material in Philippine AHBs. As discussed previously, the development of conservation material can be classified into three types depending on the purpose: (i) consolidate cracks, (ii) repair mortar for visible material loss, and (iii) replace/substitute an intensely degraded substrate. For example, Korat et al. [108] developed a mortar to repair deteriorated tuff used in AHSs in Northwest Slovenia, dating to Roman times, by mixing a binding crushed tuff and quartz sand with tetraethyl orthosilicate (TEOS), an organic silica source. The porosity of the repair mortar was higher than that of the original stones, with lower compressive strengths (3.7–8.0 MPa) from the original tuff (72–85.8 MPa), but it had similar resistance to salt weathering. Several studies preferred this high-porosity,

 doi:10.20944/preprints202603.0062.v1

low-compressive-strength material for restoration because it allowed better water transport and dehydration of the restoration material, thereby avoiding damage to the original substrate [9,28,94,99].

Meanwhile, Menningen et al. [28] developed a restoration mortar and replacement stones using cement and lime for Mexican and Armenian AHS. They found that the restoration mortar closely resembled the physical and mechanical properties, thermal expansion, hydric properties (water transport), and weathering durability of the original rock. At the same time, the aesthetic compatibility was maintained by adding colored inorganic pigments and crushed original tuff as fine and coarse aggregates. In addition, Stefanidou et al. [44] designed restoration mortars for historic monuments in Greece using cement, old stone, local clays, and inorganic pigments to maintain aesthetic compatibility, resulting in similar physico-mechanical properties and material texture. In contrast, the ancient theatre of Maronia, built from Coarse-grained Marble with a porosity of 0.8% and a compressive strength of 30.3 MPa, was restored by filling small cracks, resulting in a porosity of 12.5% and a compressive strength of 8.5 MPa, demonstrating a significant difference in physico-mechanical properties. The difference is attributed to its application, which fills small cracks in the substrate; thus, it was designed to meet the lowest mechanical limit to prevent inducing stress on the original stones. Therefore, if the purpose was to repair the deteriorated part of the stone, the resulting physical and mechanical properties should be less durable than the original stone to limit damage. In contrast, if the objective is to replace or restore stones, then a similar physico-mechanical property to the original stone is necessary.

Recently, several papers proposed different criteria for evaluating the compatibility of geopolymers, but this critical analysis section is limited to aesthetic compatibility, including color, valorization of waste, and material availability in the Philippines. To maintain the original color of the stones for geopolymers products, recent studies have added colored rocks, crushed original stones, inorganic pigments, and dyeing. However, to limit the production of trial mixtures and additional costs associated with optimizing the color of the stone upon the addition of commercially available colored pigments. For example, Menningen et al. [28] formulated several mixtures with different yellow oxide pigments prior to achieving the optimized color to match the original color of Golden Armenian Tuff. This indicates a need to utilize precursors with similar chromatic properties to the original stone, as they provide recyclability and strength beyond color. For example, Fugazzotto et al. [97,98] valorized brick waste to restore ancient bricks with an originally reddish-brown color, resulting in a slight color difference.

The paper presented several types of geopolymers, depending on the precursors (e.g., metakaolin, fly ash, slag, volcanic ash, volcanic soil, pumice, ceramic tile waste, and tuff waste). Table 16 shows the similarities between these materials and the rocks used in AHS in the Philippines, in terms of color, valorization (high, medium, low), and abundance (high, medium, low). Color is a general distinguishable color by the naked eye. Valorization can be classified as high for precursors from industrial waste and by-products, medium for precursors that are not commonly used but repurposed, and low for precursors obtained from naturally quarried sources or geological materials. Lastly, abundance refers to how commonly these materials are found and accessible in the Philippines.

Table 16. Summary of the color of geopolymer precursors similarity for Philippine tuff and coral rocks.

Type	Inherent color	Chromatic similarity to Philippine tuff	Chromatic similarity to coral rock	Degree of valorization	Abundancy in Philippines
Metakaolin	Creamy white	Yes	Yes	Low	High
Fly Ash	Grey	Yes	No	High	High
GGBS	White	Variable	Yes	High	High
Volcanic ash	Light grey	Yes	No	Medium	High
Volcanic soil (Ghaira)	Red	No	No	Medium	High
Pumice	Grey to whitish	Yes	No	Low	Low

 doi:10.20944/preprints202603.0062.v1

Ceramic	Red	No	No	High	Variable
Tuff waste	Grey	Yes	No	High	Low
Silica fume	Grey	Yes	No	High	High
Mine waste	–	–	–	High	High

7. Summary and Future Perspectives

In AHS conservation, there is a need to develop restoration materials that are environmentally acceptable, compatible, and sustainable while maintaining the aesthetic appearance of the structure. Recently, the application of geopolymers in AHS conservation as an alternative restoration material to Ordinary Portland cement is becoming more mainstream due to their low carbon footprint, reduced energy consumption, and favorable physical, mechanical, and aesthetic properties. Although several geopolymers showed potential for AHB conservation, their compatibility performance towards the original materials remains unclear.

This review provided a comprehensive overview of the different geopolymers, including the precursor materials, types of aggregates, composition of the admixture, and the resulting physical, mechanical, and aesthetic properties of the material. In addition, the analysis of compatibility criteria for natural stones used in AHBs was reviewed, focusing on aesthetic, physical, chemical, and mechanical compatibility with the original materials, indicating the importance of aesthetic compatibility as the primary criterion for restoration. Furthermore, a brief critical analysis was presented, specifically on the precursors used in the formulation of the geopolymers in terms of chromatic similarity to tuff and coral rock, the degree of valorization and sources, location relative to the structure for restoration of natural stone such as tuff and coral rock, and the primary material used in cultural heritage in the Philippines.

Metakaolin was prominently identified as an important material in geopolymer formulations, either as the main precursor or as an additive/admixture, due to its high reactivity and favorable composition. Other popular materials for geopolymer formulation include fly ash, slags, volcanic ash, volcanic soil, pumice, and ceramic and tuff waste. Meanwhile, several of the least common materials used as main precursors for geopolymers include mine waste, local clay, soils, and silica fume. For alkaline activators, sodium silicate with sodium hydroxide was commonly used, while metakaolin and fly ash were popular admixtures. Lastly, aggregate basically depended on the availability of the material, and those readily and locally available, like quartz sand, river sand, crushed stones, carbonate stones, volcanic rock, volcanic sand, tuff, brick, and ceramic aggregates have been reported

To assess compatibility criteria, several studies investigated aesthetic, physical, chemical, and mechanical compatibility. Aesthetic compatibility includes color and the presence of efflorescence, while physical compatibility is conducted to compare the physical properties of the material to those of natural stone. Chemical compatibility involves ionic release and microstructural analysis. Lastly, mechanical testing assesses the surface hardness, adhesion, compactness, and compressive and tensile strengths of the geopolymer. As the application of the material may vary during restoration, either as applied as repair mortars for patching deteriorated stones or completely substituting the original stone, the physical and mechanical properties depend on the purpose; however, aesthetic compatibility is a criterion primarily considered to be assessed to preserve the historical appearance without permanently altering the original appearance of the original material.

In the critical analysis, the aesthetic compatibility of the different geopolymers for tuff and coral rock-built structures in the Philippines was examined. It is recommended, with consideration of color, valorization, and abundance, to use fly ash, slag, and volcanic ash as precursors for the restoration of tuff-built heritage, while, for coral rock, it is recommended to use either metakaolin, slag, or local limestones to maintain compatibility.

For future perspective, due to the AHS's susceptibility to earthquakes, studies on mortar strengthening and seismic masonry resilience are recently investigating fiber-reinforced geopolymers. Additionally, compatible stone consolidants were formulated in recent years to retard

 doi:10.20944/preprints202603.0062.v1

the weathering of tuff and other stone due to extreme pollution in the modern day, innovating techniques for the preservation of the AHS while maintaining its aesthetic appearance.

Supplementary Materials: The following supporting information can be downloaded at the website of this paper posted on Preprints.org.

Author Contributions: Conceptualization, KBS, MVT, TP and CBT; methodology, KBS, RL, RO, SX, JZ, and CBT.; software, KBS, CBT.; validation, CBT., CBT and CBT.; formal analysis, KBS, RL, RO, SX, JZ, and CBT.; investigation, TP, ICM, TA, CBT.; resources TA, IP, MI, SJ, and CBT.; data curation, KBS, RL, RO, ICM, and CBT.; writing—original draft preparation KBS, MVT, and CBT; writing—review and editing, RL, RO, TP, SX, JZ, ICM, TA, IP, MI, and SJ; visualization, KBS, RL, RO, and ICM; supervision, MVT, TP, CBT; project administration, MVT, TA, IP, MI, SJ, and C.B.T.; funding acquisition, MVT, ICM, and CBT. All authors have read and agreed to the published version of the manuscript." Please turn to the CRediT taxonomy for the term explanation. Authorship must be limited to those who have contributed substantially to the work reported.

Funding: This research was supported by the Department of Science and Technology–Philippine Council for Industry, Energy, and Emerging Technology Research and Development (DOST-PCIEERD) through EPOCH Project 2 (Grant Number: 1212387) and the Department of Research of Mindanao State University-Iligan Institute of Technology (MSU-IIT), Iligan City, Philippines (SO#00228-IIT).

Data Availability Statement: The original data are contained within the Article. Further inquiries can be directed to the corresponding author.

Acknowledgments: The authors also express our sincere appreciation to the editors and anonymous reviewers for their valuable comments and to the journal's editorial team for their professional assistance. Gratitude is also extended to colleagues from Mindanao State University–Iligan Institute of Technology (MSU-IIT) for their support, and to the Department of Science and Technology–Engineering Research and Development for Technology (DOST-ERDT) program for the graduate scholarship of KBS.

Conflicts of Interest: The authors declare no conflicts of interest.

Abbreviations

The following abbreviations are used in this manuscript:

AHS	Architectural heritage structures
ASM	Artificial stone mortars
EC	Electrical conductivity
FA	Fly Ash
FRCM	Fiber reinforced cementitious materials
ICOMOS	International council on monument and sites
MK	Metakaolin
NDT	Non-destructive techniques
NHL	Natural hydraulic lime
NMF	Non-metallic fraction
OPC	Ordinary Portland cement
PCB	Printed circuit board
PM	Pumice
SEM	Scanning electron microscope
SF	Silica fume
TEOS	Tetraethyl orthosilicate
UCS	Unconfined compressive strength
UNESCO	United Nations Educational, Scientific, and Cultural Organization
UPV	Ultrasonic pulse velocity
URM	Unreinforced masonry
VA	Volcanic ash
VS	Volcanic soil
XRD	X-ray diffraction

 doi:10.20944/preprints202603.0062.v1

References

1. Siegesmund, S.; Török, Á. Building Stones. In: *Stones in Architecture: Properties and Durability*, 5th ed.; Siegesmund, S., Snethlage, R., Eds; Springer: Heidelberg, Berlin, Germany, **2014**, 11-97. https://doi.org/10.1007/978-3-642-45155-3_2
2. Pötzl, C.; Siegesmund, S.; López-Doncel, R.; Dohrmann, R. Key parameters of volcanic tuffs used as building stone: a statistical approach. *Environ. Earth Sci.* **2022,** *81*(10). https://doi.org/10.1007/s12665-021-10114-w
3. Martínez-Martínez, J.; Pola, A.; García-Sánchez, L.; Reyes Agustin, G.; Osorio Ocampo, L. S.; Macías Vázquez, J. L.; Robles-Camacho, J. Building stones used in the architectural heritage of Morelia (México): Quarries location, rock durability and stone compatibility in the monument. *Environ. Earth Sci.* **2018**, *77*(5), 167. https://doi.org/10.1007/s12665-018-7340-7
4. Di Benedetto C.; Cappelletti, P.; Favaro, M.; Graziano, S.F.; Langella, A.; Calcaterra, D.; Colella, A. Porosity as key factor in the durability of two historical building stones: Neapolitan Yellow Tuff and Vicenza Stone, *Eng. Geol.* **2015**, *193*, 310–319, https://doi.org/10.1016/j.enggeo.2015.05.006
5. Germinario, L.; Török, Á. Variability of technical properties and durability in volcanic tuffs from the same quarry region – examples from Northern Hungary. *Eng. Geol.* **2019**, 262, 105319, https://doi.org/10.1016/j.enggeo.2019.105319
6. Lubelli, B.; Nijland, T. G.; Tolboom, H.J. Moisture induced weathering of volcanic tuffstone. *Constr. Build. Mater*. **2018**, *187*, 1134–1146. https://doi.org/10.1016/j.conbuildmat.2018.08.002
7. Nijland, T. G.; Van Hees, R. P. J. The volcanic foundation of Dutch architecture: Use of Rhenish tuff and trass in the Netherlands in the past two millennia. *Heron* **2016**, *61*(2), 69–98. https://www.researchgate.net/publication/310614592_The_volcanic_foundation_of_Dutch_architecture_Use_of_Rhenish_tuff_and_trass_in_the_Netherlands_in_the_past_two_millennia
8. Siedel, H.; Rust, M.; Goth, K.; Krüger, A.; Heidenfelder, W. Rochlitz porphyry tuff (Rochlitzer Porphyrtuff): A candidate for 'Global Heritage Stone Resource' designation from Germany. *Episodes* **2019**, *42*(2), 81–91. https://doi.org/10.18814/epiiugs/2019/019007
9. Korat, L.; Mirtič, B.; Mladenovič, A.; Pranjić, A. M.; Kramar, S. Formulation and microstructural evaluation of tuff repair mortar. *J. Cult Herit* **2015**, *16*(5), 705–711. https://doi.org/10.1016/j.culher.2014.11.002
10. Cárdenes, V.; Cabrera-Guillén, D.; López-Piñeiro, S.; de Argandoña, V. G. R.; Rubio-Ordóñez, A. The Historical Significance of the Welded Tuffs from Arucas, Canary Islands. *Geoheritage* **2022**, *14*(46). https://doi.org/10.1007/s12371-022-00680-1
11. Valido, J. A.; Cáceres, J. M.; Sousa, L. M. O. Physical and mechanical properties of Ignimbrite from Arucas, Canary Islands. *Environ Earth Sci.* **2023**, *82*(13), 342. https://doi.org/10.1007/s12665-023-11024-9
12. Siegesmund, S.; Pötzl, C.; López-Doncel, R.; Gross, C. J.; Dohrmann, R.; Ufer, K. Overview and quality assessment of volcanic tuffs in the Mexican building heritage. *Environ. Earth Sci.* **2022**, *81*(17). https://doi.org/10.1007/s12665-022-10530-6
13. López-Doncel, R.; Wedekind, W.; Aguillón-Robles, A.; Dohrmann, R.; Molina-Maldonado, S.; Leiser, T.; Wittenborn, A.; Siegesmund, S. Thermal expansion on volcanic tuff rocks used as building stones: Examples from Mexico. *Environ. Earth Sci.* **2018**., 77(9). Scopus. https://doi.org/10.1007/s12665-018-7533-0
14. Ruiz-Ruiz, R.; Alonso-Guzman, E. M.; Martinez-Molina, W.; Chavez-Garcia, H. L.; Arreola-Sanchez, M.; Borrego-Perez, J. A.; Navarrete-Seras, M. A.; Velazquez-Perez, J. A.; Morales-Rosales, L. A. Environmental Decay of Ignimbrite Patrimonial Monuments in the Dry, Urban, and Non-Industrial Atmosphere of Morelia (México). *Heritage* **2023**, *6*(3), 3137–3158. https://doi.org/10.3390/heritage6030167
15. Padilla-Ceniceros, R.; Pacheco-Martínez, J.; López-Doncel, R.A.; Orenday-Tapia, E.E. Rock deterioration in the masonry walls of the Cathedral Basilica of Aguascalientes. *Mexico. Rev. Mex Cienc. Geol* **2017**. *34*, 138–139. https://doi.org/10.22201/cgeo.20072902e.2017.2.466
16. López-Doncel, R.; Wedekind, W.; Dohrmann, R.; Siegesmund, S. Moisture expansion associated to secondary porosity: An example of the Loseros Tuff of Guanajuato, Mexico. *Environ. Earth Sci.* **2013**, 69(4), 1189–1201. https://doi.org/10.1007/s12665-012-1781-1
17. González-León, L. I.; Canet, C.; Lozada-Amador, E.; Alvarado-Sizzo, I.; Lagarda-García, F. O.; Cruz-Pérez, M. Á.; García-Alonso, E.; Mora-Chaparro, J. C.; Torres, P. S. U.; Salgado-Martínez, E. Tezoantla Tuff

 doi:10.20944/preprints202603.0062.v1

(«Cantera de Tezoantla», Hidalgo state): The first Mexican "Heritage Stone." *Episodes* **2024**, *47*(1), 109–119. https://doi.org/10.18814/epiiugs/2023/023016

18. Elert, K.; Ruiz-Agudo, E.; Jroundi, F.; Gonzalez-Muñoz, M. T.; Fash, B. W.; Fash, W. L.; Valentin, N.; de Tagle, A.; Rodriguez-Navarro, C. Degradation of ancient Maya carved tuff stone at Copan and its bacterial bioconservation. Npj Mater. Degrad. **2021**, *5*(1). https://doi.org/10.1038/s41529-021-00191-4
19. Jroundi, F.; Elert, K.; Ruiz-Agudo, E.; Gonzalez-Muñoz, M. T.; Rodriguez-Navarro, C. Bacterial Diversity Evolution in Maya Plaster and Stone Following a Bio-Conservation Treatment. *Front. Microbiol.* **2020**, *11*, 599144. https://doi.org/10.3389/fmicb.2020.599144
20. Deniz, B. E.; Topal, T. A new durability assessment method of the tuffs used in some historical buildings of Cappadocia (Turkey). *Environ. Earth Sci.* **2021**, 80(7). https://doi.org/10.1007/s12665-021-09546-1
21. Çelik, M. Y.; Güven, Ö. An assessment of the durability of untreated and water repellent-treated cultural heritage stone (Döğer tuff-Turkey) by salt mist and salt crystallization tests. *Bull. Eng. Geol. Environ*. **2024**, *83*(5). https://doi.org/10.1007/s10064-024-03696-9.
22. Çelik, M. Y.; Güven, Ö. Evaluation of the Durability of Untreated and Water-Repellent-Treated Cultural Heritage Stone (Döğer Tuff-Turkey) through Capillary Water Absorption and Freeze-Thaw Tests. *Geoheritage* **2024**, *16*(4). https://doi.org/10.1007/s12371-024-01017-w
23. Çelik, M. Y.; Sert, M. The role of different salt solutions and their concentration ratios in salt crystallization test on the durability of the Döğer tuff (Afyonkarahisar, Turkey) used as building stones of cultural heritages. *Bull. Eng. Geol. Environ.* **2020**, *79*(10), 5553–5568. Scopus. https://doi.org/10.1007/s10064-020-01896-7
24. Çelik, M. Y.; Sert, M. An assessment of capillary water absorption changes related to the different salt solutions and their concentrations ratios in the Döğer tuff (Afyonkarahisar-Turkey) used as building stone of cultural heritages. *J. Build. Eng.* **2021**, 35. Scopus. https://doi.org/10.1016/j.jobe.2020.102102
25. Çelik, M. Y.; Sert, M. An investigation of the pore size distribution variations with salt crystallization tests of Döğer tuff (Afyonkarahisar-Turkey). *Bull. Eng. Geol. Environ.* **2022**, *81*(1). https://doi.org/10.1007/s10064-021-02549-z
26. Maras, M. M.; Kose, M. M.; Rızaoglu, T. Microstructural characterization and mechanical properties of volcanic tuff (Malatya, turkey) used as building stone for the restoring cultural heritage. Period. *Polytechn. Civ. Eng.* **2020**, *65*(1), 309–319. https://doi.org/10.3311/PPci.16977
27. Pötzl, C.; Siegesmund, S.; Dohrmann, R.; Koning, J. M.; Wedekind, W. Deterioration of volcanic tuff rocks from Armenia: Constraints on salt crystallization and hydric expansion. *Environ. Earth Sci.* **2018**, 77(19). https://doi.org/10.1007/s12665-018-7777-8
28. Menningen, J.; Klein, C.; Pötzl, C.; Gross, C. J.; Siegesmund, S. Development of restoration mortars and artificial stones for use in restoring cultural heritage sites made from volcanic tuffs. *Environ. Earth Sci.* **2022**, *81*(20). https://doi.org/10.1007/s12665-022-10607-2.
29. Guo, X.; Zhang, Y.; Xu, X.; Dai, S. Petrographic and geochemical analyses to characterise the source of built historical natural stones—A case study of the volcanic stones from historical quarries and Baoguosi Temple in the city of Ningbo, China. *Built herit.* **2023**, 7(1). https://doi.org/10.1186/s43238-023-00091-3
30. Wu, Y.; Shen, J.; Zhang, J.; Zhang, B. Environmental Factor Accelerate the Deterioration of Tuff Stone Heritage: A Case Study of a Stone House in Southeast China. *Buildings* **2022**, 12(2). Scopus. https://doi.org/10.3390/buildings12020188
31. Jo, Y. H.; Lee, C. H. Weathering features of a five-story stone pagoda compared to its quarrying site in Geumgolsan Mountain, Korea. *Environ Earth Sci.* **2022**, *81*(6). https://doi.org/10.1007/s12665-022-10303-1
32. Germinario, L.; Oguchi, C. T. Gypsum, mirabilite, and thenardite efflorescences of tuff stone in the underground environment. *Environ. Earth Sci.* **2022**, *81*(242). https://doi.org/10.1007/s12665-022-10344-6
33. Germinario, L.; Oguchi, C. T. Underground salt weathering of heritage stone: Lithological and environmental constraints on the formation of sulfate efflorescences and crusts. *J. Cult. Herit.* **2021**, *49*, 85–93. Scopus. https://doi.org/10.1016/j.culher.2021.02.011
34. Manohar, S., Bala, K., Santhanam, M., Menon, A. Characteristics and deterioration mechanisms in coral stones used in a historical monument in a saline environment. *Constr. Build. Mater.* **2020**, 241. https://doi.org/10.1016/j.conbuildmat.2020.118102.

 doi:10.20944/preprints202603.0062.v1

35. Meng, Q.; Dong, Y.; Li, H.; Cui, L. Static and dynamic compressive performance of coral reef limestone: Interpretations of rate effect from laboratory tests. *Bull. Eng. Geol. Environ.* **2024**, 83(5), 194. https://doi.org/10.1007/s10064-024-03700-2
36. Xu, J., Huang, X., Zhang, Z.; Jin, G. Pore structure characteristics of coral reef limestone: A combined polarizing microscope and CT scanning study. In Proceedings of Geo Shanghai International Conference 2024 - Volume 3: Transportation Geotechnics, Shanghai, China, 26 May. https://doi.org/10.1088/1755-1315/1332/1/012026
37. Wei, X.; Luo, Y.; Tao, Y.; Li, X.; Meng, F. Experimental Research into the Uniaxial Compressive Strength of Low-Density Reef Limestone Based on Image Recognition. *Materials* **2023**, *16*(15), 5465. https://doi.org/10.3390/ma16155465
38. Siegesmund, S.; Gross, C. J.; Dohrmann, R.; Marler, B.; Ufer, K.; Koch, T. Moisture expansion of tuff stones and sandstones. *Environ. Earth Sci.* **2023**, *82*(6). https://doi.org/10.1007/s12665-023-10809-2
39. Urbina Leonor, L. M.; Sosa Echeverría, R.; Alarcón Jiménez, A. L.; Solano Murillo, M.; Pérez, N. A.; Sánchez Alvarez, P.; Hernández Tellez, J.; Vega, E.; Kahl, J. D. W. Wet Atmospheric Deposition Damage on Coral Limestone: An Assessment for Conservation Purposes. *Geoheritage* **2025**, *17*(2), 79. https://doi.org/10.1007/s12371-025-01122-4
40. Blows, J. F.; Carey, P. J.; Poole, A. B. Preliminary investigations into Caen Stone in the UK; its use, weathering and comparison with repair stone. *Build. Environ.* **2003**, *38*(9-10), 1143-1149. https://doi.org/10.1016/S0360-1323(03)00075-1
41. Přikryl, R.; Török, Á. Natural stones for monuments: their availability for restoration and evaluation. *Geol. Soc. Spec. Publ*. **2010**, 333, 1 – 9. https://doi.org/10.1144/SP333.1
42. Rozenbaum, O.; Barbanson, L.; Muller, F.; Bruand, A. Significance of a combined approach for replacement stones in the heritage buildings' conservation frame. *C. R. Geosci.* **2008**, *340*(6), 345-355, https://doi.org/10.1016/j.crte.2008.04.005
43. Török, Á.; Vogt, T.; Löbens, S.; Forgó, L. Z.; Siegesmund, S.; Weiss, T. Weathering forms of rhyolite tuffs. *Zeitschrift der Deutschen Gesellschaft für Geowissenschaften* **2005**, 177-187. https://doi.org/10.1127/1860-1804/2005/0156-0177
44. Stefanidou, M.; Pachta, V.; Papayianni, I. Design and testing of artificial stone for the restoration of stone elements in monuments and historic buildings. *Constr. Build. Mater.* **2015**, *93*, 957-965, https://doi.org/10.1016/j.conbuildmat.2015.05.063
45. Giacobello, F.; Ielo, I.; Belhamdi, H.; Plutino, M. R. Geopolymers and Functionalization Strategies for the Development of Sustainable Materials in Construction Industry and Cultural Heritage Applications: A Review. *Materials* **2022**, *15*(5). https://doi.org/10.3390/ma15051725
46. Abulencia, A. B.; Villoria, M. B. D.; Libre, R. G. D.; Jr., Quiatchon, P. R. J.; Dollente, I. J. R.; Guades, E. J.; Promentilla, M. A. B., Garciano, L. E. O.; Ongpeng, J. M. C. Geopolymers as Sustainable Material for Strengthening and Restoring Unreinforced Masonry Structures: A Review. *Buildings* **2021**, 11(11), 532. https://doi.org/10.3390/buildings11110532
47. Cong, P.; Cheng, Y. Advances in geopolymer materials: A comprehensive review. *J. Traffic Transp. Eng.* **2021**, *8*(3), 283-314. https://doi.org/10.1016/j.jtte.2021.03.004
48. Matsimbe, J.; Dinka, M.; Olukanni, D.; Musonda, I. Geopolymer: A Systematic Review of Methodologies. *Materials* **2022**, *15*(19):6852. https://doi.org/10.3390/ma15196852
49. Singh, N.B.; Middendorf, B. Geopolymers as an alternative to Portland cement: An overview. *Constr. Build Mater.* **2020**. *237*, https://doi.org/10.1016/j.conbuildmat.2019.117455
50. Amar, M.; Ladduri, B.; Alloul, A.; Benzerzour, M.; Abriak, N. Microstructure and mechanical properties of geopolymers utilizing excavated soils, metakaolin and slags. *J. Build. Eng* **2024**, *86*, https://doi.org/10.1016/j.jobe.2024.108755
51. Elert, K.; Rodriguez-Navarro, C. Degradation and conservation of clay-containing stone: A review. Construction and Building *Materials* **2022**, *330*. https://doi.org/10.1016/j.conbuildmat.2022.127226
52. Moher, D.; Liberati, A.; Tetzlaff, J.; Altman, D.G. Preferred reporting items for systematic reviews and meta-analyses: The PRISMA statement. BMJ **2009**, 339, b2535. https://doi.org/10.1136/bmj.b2535

 doi:10.20944/preprints202603.0062.v1

53. Andrews, R. The place of systematic reviews in education research. *Br. J. Educ. Stud.* **2005**, *53*, 399–416. https://doi.org/10.1111/j.1467-8527.2005.00303.x
54. Jindal-Snape, D.; Hannah, E.F.S.; Cantali, D.; Barlow, W.; MacGillivray, S. Systematic literature review of primary–secondary transitions: International research. *Rev. Educ.* **2020**, *8*, 526–566. https://doi.org/10.1002/rev3.3197.
55. Pradines, S.; Balestra, F. Excavations on the Coral Mosques of the Maldives. *J. Mater. Cult. Muslim World* **2021**, *2*(1–2), 200–226. https://doi.org/10.1163/26666286-12340022
56. Cayme, J.M.C. Chemistry of Lime Mortared Rubble Masonry in Bohol, Philippines. Int. J. Conserv. Sci. **2021**, *12* (3), 997-986, https://ijcs.ro/public/IJCS-21-72_Cayme.pdf
57. Abdel–Aty, Y. Y.; Mahmoud, H. S.; Al-Zahrani, A. A. Experimental Evaluation of Consolidation Techniques of Fossiliferous Limestone in Masonry Walls of Heritage Buildings at Historic Jeddah, Kingdom of Saudi Arabia. *Adv. Res. Conserv. Sci.* **2020**, *1*(1), 16–33. https://doi.org/10.21608/arcs.2020.111205
58. Cassar, J.; Cefai, S.; Grima, R.; Stroud, K. Sheltering archaeological sites in Malta: Lessons learnt. *Herit. Sci.* **2018**, *6*(1), 36. https://doi.org/10.1186/s40494-018-0201-6
59. Moradi, Z. The role of coral in art and architecture: An overview. *Int. J. Aquat. Biol.* (2016)., *4*(2), 125–142. https://doi.org/10.7508/ijab.2016.02.008
60. Pradines, S. The 'Trees from the Sea' Coral Architectures and Indian Ocean Maritime Resources. *J. Res. Archit. Plan.* **2024**, *34*(1), 01–17. https://doi.org/10.53700/jrap3412024_1
61. Ali, B. S.; Castro, J. J.; Omi, S.; Nazimi, K. Preserving the Past: Investigating Zanzibar's Ancient Construction Materials for Sustainable Heritage Conservation. *Buildings* **2024**, *14*(7), 2129. https://doi.org/10.3390/buildings14072129
62. Xiaoli Ji; Xiangbo Huang; Shiyun Zhong; Junli Zhou. Advancing toward a low-carbon infrastructure: Emission reduction potential of geopolymer road maintenance. *Mater. Today Sustain* **2025**, *30*, 101121, https://doi.org/10.1016/j.mtsust.2025.101121
63. Wong, L.S. Durability Performance of Geopolymer Concrete: A Review, *Polymers* **2022**, *14* (5), 868. https://doi.org/10.3390/polym14050868
64. Opiso, E.M.; Tabelin, C.B.; Maestre, C.V.; Aseniero, J.P.J.; Arima, T.; Villacorte-Tabelin, M. Utilization of Palm Oil Fuel Ash (POFA) as an Admixture for the Synthesis of a Gold Mine Tailings-Based Geopolymer Composite. *Minerals* **2023**, *13*(2), 232. https://doi.org/10.3390/min13020232
65. Opiso, E.M.; Tabelin, C.B., Maestre, C.V.; Aseniero, J.P.J.; Park, I.; Villacorte-Tabelin, M. Synthesis and characterization of coal fly ash and palm oil fuel ash modified artisanal and small-scale gold mine (ASGM) tailings based geopolymer using sugar mill lime sludge as Ca-based activator. *Heliyon* **2021,** *7*(4). https://doi.org/10.1016/j.heliyon.2021.e06654
66. Aseniero, J.P.J.; Opiso, E.M.; Banda M.H.T.; Tabelin, C.B. Potential utilization of artisanal gold-mine tailings as geopolymeric source material: preliminary investigation. *SN Appl. Sci.* **2019**, *1*(35). https://doi.org/10.1007/s42452-018-0045-4
67. Mabroum, S; Moukannaa, S.; El Machi, A.; Taha, Y.; Benzaazoua, M.; Hakkou, R. Mine wastes based geopolymers: A critical review. *Clean. Eng. Technol* **2020,** *1*. https://doi.org/10.1016/j.clet.2020.100014
68. Allali, F.; Joussein, E.; Kandri, N. I.; Rossignol, S. The influence of calcium content on the performance of metakaolin-based geomaterials applied in mortars restoration. *Mater. Des.* **2016**., *103*, 1–9. https://doi.org/10.1016/j.matdes.2016.04.028
69. Clausi, M.; Tarantino, S. C.; Magnani, L. L.; Riccardi, M. P.; Tedeschi, C.; Zema, M. Metakaolin as a precursor of materials for applications in Cultural Heritage: Geopolymer-based mortars with ornamental stone aggregates. *Appl. Clay Sci.* **2016**, 132–133, 589–599. Scopus. https://doi.org/10.1016/j.clay.2016.08.009
70. Ricciotti, L.; Molino, A. J.; Roviello, V.; Chianese, E.; Cennamo, P.; Roviello, G. Geopolymer composites for potential applications in cultural heritage. *Environments* **2017**, 4(4), 1–15. https://doi.org/10.3390/environments4040091
71. Moutinho, S.; Costa, C.; Cerqueira, Â.; Rocha, F.; Velosa, A. Geopolymers and polymers in the conservation of tile facades. *Constr. Build. Mater.* **2019**, 197, 175–184. https://doi.org/10.1016/j.conbuildmat.2018.11.058

 doi:10.20944/preprints202603.0062.v1

72. Moutinho, S.; Costa, C.; Andrejkovičová, S.; Mariz, L.; Sequeira, C.; Terroso, D.; Rocha, F.; Velosa, A. Assessment of properties of metakaolin-based geopolymers applied in the conservation of tile facades. *Constr. Build. Mater.* **2020**, *259*. https://doi.org/10.1016/j.conbuildmat.2020.119759
73. Mácová, P.; Sotiriadis, K.; Slížková, Z.; Šašek, P.; Řehoř, M.; Závada, J. Evaluation of Physical Properties of a Metakaolin-Based Alkali-Activated Binder Containing Waste Foam Glass. *Materials* **2020**, *13*(23), 5458. https://doi.org/10.3390/ma13235458
74. Perná, I.; Novotná, M.; Řimnáčová, D.; Šupová, M. New Metakaolin-Based Geopolymers with the Addition of Different Types of Waste Stone Powder. *Crystals* **2021**, *11*(8), 983. https://doi.org/10.3390/cryst11080983
75. Ricciotti, L.; Occhicone, A.; Manzi, S.; Saccani, A.; Ferone, C.; Tarallo, O.; Roviello, G. Sustainable Materials Based on Geopolymer–Polyvinyl Acetate Composites for Art and Design Applications. *Polymers* **2022**, *14*(24). https://doi.org/10.3390/polym14245461
76. Angelo, A. D.; Arconati, V.; Vertuccio, L.; Viola, V.; Catauro, M. Use of Organic Dyes to Color the Metakaolin-Based Geopolymer: A Physico-Chemical Characterization. *Macromol. Symp.* **2023**, *411*(1). https://doi.org/10.1002/masy.202200145
77. Perná, I.; Novotná, M.; Hanzlíček, T.; Rafl, J.; Nováková, M. The application of geopolymers in the renovation of the historical ceramic tiles in the pilgrimage church of St. John of Nepomuk (Czech Republic). *Case Stud. Constr. Mater.* **2025**, *22*, https://doi.org/10.1016/j.cscm.2024.e04161
78. Perná, I.; Novotná, M.; Hanzlíček, T.; Šupová, M.; Řimnáčová, D. Metakaolin-based geopolymer formation and properties: The influence of the maturation period and environment (air, demineralized and sea water). *J. Ind. Eng. Chem.* **2024**, *134*, 415–424. https://doi.org/10.1016/j.jiec.2024.01.005
79. Jin, G.; Wang, X.; Mao, H.; Ji, S.; Shi, Q. Preparation and properties of metakaolin-fumed-silica geopolymer modified with sodium silicate and potassium silicate activators. *Chin. J. Anal. Chem.* **2024**, *52*(1), 100352. https://doi.org/10.1016/j.cjac.2023.100352
80. Singh, N. B. Fly Ash-Based Geopolymer Binder: A Future Construction Material. *Minerals* **2018**, *8*(7), 299. https://doi.org/10.3390/min8070299
81. Kakria, K.; Thirumalini, S.; Secco, M.; Shanmuga Priya, T. A novel approach for the development of sustainable hybridized geopolymer mortar from waste printed circuit boards. *Resour. Conserv. Recycl.* **2020**, *163*, 105066. https://doi.org/10.1016/j.resconrec.2020.105066
82. Dollente, I. J. R.; Valerio, D. N. R.; Quiatchon, P. R. J.; Abulencia, A. B.; Villoria, M. B. D.; Garciano, L. E. O.; Promentilla, M. A. B.; Guades, E. J.; Ongpeng, J. M. C. Enhancing the Mechanical Properties of Historical Masonry Using Fiber-Reinforced Geopolymers. *Polymers* **2023**, *15*(4). https://doi.org/10.3390/polym15041017
83. Longo, F.; Cascardi, A.; Lassandro, P.; Aiello, M. A. A new Fabric Reinforced Geopolymer Mortar (FRGM) with mechanical and energy benefits. *Fibers* **2020**, *8*(8). https://doi.org/10.3390/FIB8080049
84. Vasanelli, E.; Calò, S.; Cascardi, A.; Aiello, M. A. The Use of Lightweight Aggregates in Geopolymeric Mortars: The Effect of Liquid Absorption on the Physical/Mechanical Properties of the Mortar. *Materials* **2024**, *17*(8), 1798. https://doi.org/10.3390/ma17081798
85. Tamburini, S.; Natali, M.; Garbin, E.; Panizza, M.; Favaro, M.; Valluzzi, M. R. Geopolymer matrix for fibre reinforced composites aimed at strengthening masonry structures. *Constr. Build. Mater.* **2017**, *141*, 542–552. https://doi.org/10.1016/j.conbuildmat.2017.03.017
86. Maras, M. M. Characterization of performable geopolymer mortars for use as repair material. *Struct. Concr.* **2021**, *22*(5), 3173–3188. Scopus. https://doi.org/10.1002/suco.202100355
87. Gupta, V.; Pathak, D. K.; Kumar, R.; Miglani, A.; Siddique, S.; Chaudhary, S. Production of colored bi-layered bricks from stone processing wastes: Structural and spectroscopic characterization. *Constr. Build. Mater.* **2021**, *278*, 122339. https://doi.org/10.1016/j.conbuildmat.2021.122339
88. Kutlusoy, E.; Maras, M. M.; Ekinci, E.; Rihawi, B. Production parameters of novel geopolymer masonry mortar in heritage buildings: Application in masonry building elements. *J. Build. Eng.* **2023**, 76. https://doi.org/10.1016/j.jobe.2023.107038
89. Finocchiaro, C.; Barone, G.; Mazzoleni, P.; Leonelli, C.; Gharzouni, A.; Rossignol, S. FT-IR study of early stages of alkali activated materials based on pyroclastic deposits (Mt. Etna, Sicily, Italy) using two different alkaline solutions. *Constr. Build. Mater.* **2020**, 262, 120095. https://doi.org/10.1016/j.conbuildmat.2020.120095

 doi:10.20944/preprints202603.0062.v1

90. Occhipinti, R.; Caggiani, M. C.; Andriulo, F.; Barone, G.; de Ferri, L., Mazzoleni, P. Effect of atmospheric exposure on alkali activated binders and mortars from Mt. Etna volcanic precursors. *Mater. Lett.* **2022**, *315*. https://doi.org/10.1016/j.matlet.2022.131940
91. Finocchiaro, C.; Occhipinti, R.; Barone, G.; Mazzoleni, P.; Andreola, F.; Romagnoli, M.; Leonelli, C. Effects of the addition of slaked lime to alkali-activated pastes based on volcanic ashes from Mt. Etna volcano (Italy). *Ceram. Int.* **2024**., *50*(13), 24479–24486. https://doi.org/10.1016/j.ceramint.2024.04.181
92. Occhipinti, R.; Caggiani, M. C.; De Ferri, L.; Xu, Z.; Steindal, C. C.; Razavi, N.; Andriulo, F.; Mazzoleni, P.; Barone, G. Structural properties of volcanic precursors-based geopolymers before and after natural weathering. *Ceram. Int.* **2023**, 49(13), 21892–21902. https://doi.org/10.1016/j.ceramint.2023.04.013
93. Occhipinti, R.; Lanzafame, G.; Lluveras Tenorio, A.; Finocchiaro, C.; Gigli, L.; Tinè, M. R.; Mazzoleni, P.; Barone, G. Design of alkali activated foamy binders from Sicilian volcanic precursors. *Ceram. Int.* **2023**, 49(23), 38835–38846. https://doi.org/10.1016/j.ceramint.2023.09.220
94. Occhipinti, R.; Stroscio, A.; Finocchiaro, C.; Fugazzotto, M.; Leonelli, C.; José Lo Faro, M.; Megna, B.; Barone, G.; Mazzoleni, P. Alkali activated materials using pumice from the Aeolian Islands (Sicily, Italy) and their potentiality for cultural heritage applications: Preliminary study. *Constr. Build. Mater.* **2020**, *259*. https://doi.org/10.1016/j.conbuildmat.2020.120391
95. Ricciotti, L.; Occhicone, A.; Ferone, C.; Cioffi, R.; Tarallo, O.; Roviello, G. Development of Geopolymer-Based Materials with Ceramic Waste for Artistic and Restoration Applications. *Materials* **2022**, *15*(23). https://doi.org/10.3390/ma15238600
96. Fugazzotto, M.; Mazzoleni, P.; Lancellotti, I.; Camerini, R.; Ferrari, P.; Tiné, M.; Centauro, I.; Salvatici, T.; Barone, G. Industrial Ceramics: From Waste to New Resources for Eco-Sustainable Building Materials. *Minerals* **2023**, *13*(6), 815. https://doi.org/10.3390/min13060815
97. Fugazzotto, M.; Barone, G.; Mazzoleni, P. Mortars Produced by Alkaline Activation of Construction Ceramic Waste: Suitability Assessment within Conservation Issue. Int. J. Archit. Herit **2024**. https://doi.org/10.1080/15583058.2024.2396987
98. Fugazzotto, M.; Mazzoleni, P.; Stroscio, A.; Barone, G. Creating Mortars through the Alkaline Activation of Ceramic Waste from Construction: Case Studies on Their Applicability and Versatility in Conservation. *Sustainability* **2024**, *16*(3). https://doi.org/10.3390/su16031085
99. Capasso, I.; D'Angelo, G.; Fumo, M.; del Rio Merino, M.; Caputo, D.; Liguori, B. Valorisation of Tuff and Brick Wastes by Alkali Activation for Historical Building Remediation. *Materials* **2023**, *16*(20). https://doi.org/10.3390/ma16206619
100. Baltazar, L. G. Performance of Silica Fume-Based Geopolymer Grouts for Heritage Masonry Consolidation. *Crystals* **2022**, *12*(2). https://doi.org/10.3390/cryst12020288
101. Beghoura, I.; Castro-Gomes, J.; Ihsan, H.; Estrada, N. Feasibility of alkali-activated mining waste foamed materials incorporating expanded granulated cork. *Min. Sci.* **2017**. https://doi.org/10.5277/MSC172401
102. Rescic, S.; Mattone, M.; Fratini, F.; Luvidi, L. Earthen plasters stabilized through sustainable additives: An experimental campaign. *Sustainability* **2021**, *13*(3), 1–31. https://doi.org/10.3390/su13031090
103. Geraldes, C. F. M.; Lima, A. M.; Delgado-Rodrigues, J.; Mimoso, J. M.; Pereira, S. R. M. Geopolymers as potential repair material in tiles conservation. *Appl. Phys A.* **2016**, 122(3), 197. https://doi.org/10.1007/s00339-016-9709-3
104. Pappalardo, G.; Mineo, S.; Caliò, D.; Bognandi, A. Evaluation of Natural Stone Weathering in Heritage Building by Infrared Thermography. *Heritage* **2022**, *5*(3), 2594–2614. https://doi.org/10.3390/heritage5030135.
105. Salami, B.; Oyehan, T., Gambo, Y.; Badmus, S.; Tanimu, G.; Adamu, S.; Lateef, S.; Saleh, T. Technological trends in nanosilica synthesis and utilization in advanced treatment of water and wastewater. *Environ. Sci. Pollut. Res.* **2022**, *29*. https://doi.org/10.1007/s11356-022-19793-9
106. Vasanelli, E.; Calò, S.; Cascardi, A.; Aiello, M. A. The Use of Lightweight Aggregates in Geopolymeric Mortars: The Effect of Liquid Absorption on the Physical/Mechanical Properties of the Mortar. *Materials* **2024**., *17*(8), 1798. https://doi.org/10.3390/ma17081798

 doi:10.20944/preprints202603.0062.v1

107. The Geology of Guadalupe Tuff. UP Geological Society E-Bedrock, UP Geological Society **2021**. Available Online: https://medium.com/up-geological-society-e-bedrock/the-geology-of-the-guadalupe-tuff-2ecdb187f55a (Accessed on Nov 2025)
108. Korat, L.; Mirtič, B.; Mladenovič, A.; Pranjić, A. M.; Kramar, S. Formulation and microstructural evaluation of tuff repair mortar. J. Cult. Herit **2015**, *16*(5), 705–711. https://doi.org/10.1016/j.culher.2014.11.002
109. Heap, M. J.; Farquharson, J. I.; Kushnir, A. R. L.; Lavallée, Y.; Baud, P.; Gilg, H. A.; Reuschlé, T. The influence of water on the strength of Neapolitan Yellow Tuff, the most widely used building stone in Naples (Italy). *Bull. Volcanol.* **2018**, 80(6), 51. https://doi.org/10.1007/s00445-018-1225-1
110. Azevedo, A.R.G.; Vieira, C.M.F.; Ferreira, W.M.; Faria, K.C.P.; Pedroti, L.G.; Mendes, B.C. Potential use of ceramic waste as precursor in the geopolymerization reaction for the production of ceramic roof tiles. *J. Build. Eng.* **2020**, https://doi.org/10.1016/j.jobe.2019.101156
111. Ministero per i beni e le attività culturali Roma, Giugno 2004. Code of Cultural and Landscape Heritage. Available Online: https://www.eui.eu/Projects/InternationalArtHeritageLaw/Documents/NationalLegislation/Italy/itculturallandscapeheritge2004engtof.pdf (Accessed on Nov. 2025)
112. Fourteenth (14th) Congress. Republic of the Philippines. Republic Act No. 10066. An act providing for the protection and conservation of the national cultural heritage, strengthening the national commission for culture and the arts (NCCA) and its affiliated cultural agencies, and for other purposes. Availabl Online: https://lawphil.net/statutes/repacts/ra2010/ra_10066_2010.html (Accessed on Nov. 2025)
113. Jo, Y. H.; Lee, C. H. Weathering features of a five-story stone pagoda compared to its quarrying site in Geumgolsan Mountain, Korea. *Environ. Earth Sci.* **2022**, *81*(6). https://doi.org/10.1007/s12665-022-10303-1
114. Liu, J.; Xie, G.; Wang, Z.; Li, Z.; Fan, X.; Jin, H.; Zhange, W.; Xing, F.; Tang, L. Synthesis of geopolymer using municipal solid waste incineration fly ash and steel slag: Hydration properties and immobilization of heavy metals. *J. Environ. Manag.* **2023**, *341*, 118053. https://doi.org/10.1016/j.jenvman.2023.118053
115. Lei, Z.; Pavia, S. Geopolymer based on biomass ash from agricultural residues. *Constr. Build Mater.* **2024**., *441*, 137471. https://doi.org/10.1016/j.conbuildmat.2024.137471
116. Lucero, R., Jr.; Salisid, K. B.; Oros, R.; Bongabong, A.; Alguno, A.; Villacorte-Tabelin, M.; Silwamba, M.; Phengsaart, T.; Tabelin, C. B. Nanosilica-Based Hybrid Hydrophobic Coatings for Stone Heritage Conservation: An Overview. *Minerals* **2025**, 15(11), 1134. https://doi.org/10.3390/min15111134.
117. Eang, K.E.; Igarashi, T.; Fujinaga, R.; Kondo, M.; Tabelin, C.B. Groundwater monitoring of an open-pit limestone quarry: Water-rock interaction and mixing estimation within the rock layers by geochemical and statistical analysis. *Int. J. Min. Sc. Technol.* **2018,** *28*, 849-857. https://doi.org/10.1016/j.ijmst.2018.04.002
118. Dahan, A.M.E.; Alorro, R.D.; Pacaña, M.L.C.; Baute, R.M.; Silva, L.C.; Tabelin, C.B.; Resabal, V.J.T. Hydrochloric Acid Leaching of Philippine Coal Fly Ash: Investigation and Optimisation of Leaching Parameters by Response Surface Methodology (RSM). *Sustain. Chem.* **2022**, *3*(1), 76-91. https://doi.org/10.3390/suschem3010006
119. Pacaña, M.L.C.; Ranay, K.A.; Tabelin, C.B.; Alorro, R.D.; Resabal, V.J.T. Optimization of Mixed Mineral–Organic Acid Leaching for Critical Rare Earth Element Extraction from Philippine Coal Fly Ash. *Sustainability* **2025**, *17*(24), 11076. https://doi.org/10.3390/su172411076
120. Tabelin, C.B.; Igarashi, T.; Arima, T.; Sato, D.; Tatsuhara, T.; Tamoto, S. Characterization and evaluation of arsenic and boron adsorption onto natural geologic materials, and their application in the disposal of excavated altered rock. *Geoderma* **2014**, *213*, 163–172. https://doi.org/10.1016/j.geoderma.2013.07.037
121. Tabelin, C.B.; Igarashi, T.; Yoneda, T.; Tamamura, S. Utilization of natural and artificial adsorbents in the mitigation of arsenic leached from hydrothermally altered rock. *Eng. Geol.* **2013**, *156*, 58–67. https://doi.org/10.1016/j.enggeo.2013.02.001
122. The Philippine Registry of Heritage (PRH), Talampamana ng Pilipinas. Available Online: https://talapamana.ncca.gov.ph (Accessed on Jan 2026)
123. National Museum of The Philippines (NMP). Annual Report 2021. Available online: https://weblinks.nationalmuseum.gov.ph/wp-content/uploads/2023/01/30111112/NMP-FY-2021-Annual-Report_compressed.pdf. (Accessed on Jan 2026)

 doi:10.20944/preprints202603.0062.v1

Disclaimer/Publisher's Note: The statements, opinions and data contained in all publications are solely those of the individual author(s) and contributor(s) and not of MDPI and/or the editor(s). MDPI and/or the editor(s) disclaim responsibility for any injury to people or property resulting from any ideas, methods, instructions or products referred to in the content.